

# A celestial matryoshka: Dynamical and spectroscopic analysis of the Albireo system

Ronald Drimmel,<sup>1\*</sup> Alessandro Sozzetti,<sup>1</sup> Klaus-Peter Schröder,<sup>2,3</sup> Ulrich Bastian,<sup>4</sup>  
Matteo Pinamonti,<sup>1</sup> Dennis Jack<sup>2</sup> and Missael A. Hernández Huerta<sup>2</sup>

<sup>1</sup>*Istituto Nazionale di Astrofisica, Osservatorio Astrofisico di Torino, Via Osservatorio 20, 10024 Pino Torinese (TO), Italy*

<sup>2</sup>*Departamento de Astronomía, Universidad de Guanajuato, Callejón de Jalisco S/N, 36023 Guanajuato, GTO, Mexico*

<sup>3</sup>*Sterrewacht Leiden, University of Leiden, P.O. Box 9513, NL-2300 RA, Leiden, The Netherlands*

<sup>4</sup>*Zentrum für Astronomie (Center for Astronomy), Heidelberg University, Mönchhofstr. 14, D-69120 Heidelberg, Germany*

Accepted XXX. Received YYY; in original form ZZZ

## ABSTRACT

We present a spectroscopic characterisation and a new orbital solution for the binary system  $\beta$  Cyg Aa/Ac (MCA 55), the primary component ( $\beta$  Cyg A) of the well-known wide double star Albireo. By matching evolutionary tracks to the physical parameters of all three Albireo stars ( $\beta$  Cyg Aa, Ac and B) as obtained from a spectroscopic analysis of TIGRE and IUE spectra, we confirm that they are likely coeval. Our final orbit solution is based on radial-velocity measurements taken over a baseline exceeding 120 years, combined with relative astrometry from speckle interferometric observations and the absolute astrometry from the HIPPARCOS and *Gaia* missions. Our final orbit solution has a period of  $121.45^{+2.80}_{-2.73}$  years with an eccentricity of  $0.20^{+0.01}_{-0.02}$ . Thanks to the inclusion of the absolute astrometry, we find a mass ratio of  $q = 1.25^{+0.19}_{-0.16}$ , and a total mass of  $14.17^{+9.27}_{-5.19} M_{\odot}$ , indicating that the secondary (Ac) is the more massive of the pair. These results strongly suggest the presence of a fourth, unseen, member of the Albireo system. Given the current photometric data it is likely that  $\beta$  Cyg A is itself a hierarchical triple, possibly harbouring a black hole companion. We also derive the systemic proper motion, line-of-sight velocity, and an orbital parallax of the  $\beta$  Cyg A system, allowing us to quantitatively assess the hypothesis that Albireo A and B form a physically bound and genealogically connected system. Finally, we find four potential members of a common proper motion group with Albireo, though none anywhere as close by as the Albireo components A to B.

**Key words:** binaries: general — stars: individual: Albireo (or  $\beta$  Cyg) — methods: numerical — techniques: radial velocities — techniques: high angular resolution — astrometry

## 1 INTRODUCTION

Albireo ( $\beta$  Cyg) is a well-known naked-eye object that is a popular target for amateur astronomers, as it is easily resolved into a beautiful pair of stars with starkly contrasting colors. The binary nature of  $\beta$  Cyg AB has been the subject of a long-standing debate which many hoped *Gaia* astrometry would finally resolve, but the *Gaia* DR2 parallaxes for both stars are too uncertain to settle the question and, in any case, cannot be considered reliable given the brightness of the two components (Drimmel et al. 2019). Meanwhile, the *Gaia* DR2 proper motions for  $\beta$  Cyg A and B are completely different, suggesting that the pair is only a casual double. However, as pointed out by Bastian & Anton (2018), the primary  $\beta$  Cyg A is itself an unresolved binary for *Gaia* (at least up to *Gaia* DR2), and the orbital motion of the brighter component does significantly contribute to the measured proper motion of  $\beta$  Cyg A, given the short baseline of the observations contributing to the *Gaia* DR2 astrometry, so that  $\beta$  Cyg AB may still be a bound triple system. Only once the orbit of the close pair  $\beta$  Cyg A (Aa,Ac) is well determined can one hope to "correct"

the measured proper motions of  $\beta$  Cyg A to arrive at the systemic motion of  $\beta$  Cyg A and, in turn, its possible physical connection to  $\beta$  Cyg B.

The binary nature of  $\beta$  Cyg A has long been known: Given its brightness,  $\beta$  Cyg A was an obvious target for the first spectroscopic observations, and it was soon recognized as having a composite spectrum (Maury & Pickering 1897; Clerke 1899) with a dominant "cool" stellar component but clear evidence of a fainter "hot" component. More recent studies have determined the spectra as being a K3II giant with a B9V companion (Markowitz 1969; Parsons & Ake 1998). As one of the first recognized bright unresolved doubles,  $\beta$  Cyg A became a target of interest in many of the earliest spectroscopic observing programs. But due to the long orbital period and small radial-velocity amplitude, no orbital solution based on its radial velocities has been published to date.

Previous to this work, available orbit solutions of  $\beta$  Cyg A have been based solely on speckle observations measuring the relative astrometry of Aa/Ac, taken on a semiregular basis since 1976 by different observing programs. Preliminary orbit solutions were first presented by Hartkopf (1999) ( $P = 96.84$  yrs), followed by Scardia et al. (2007) ( $P = 213.859$  yrs).

\* E-mail: ronald.drimmel@inaf.it (RD)

Using the orbit solution by Scardia et al. (2007), together with the extant astrometry from HIPPARCOS and *Gaia*, Bastian & Anton (2018) argued that the inferred systemic proper motion of the  $\beta$  Cyg A system would be inconsistent with the proper motion of  $\beta$  Cyg B, making  $\beta$  Cyg AB a casual (optical) double. But their analysis also implied an implausibly small mass for the  $\beta$  Cyg A primary. However, more recently Jack et al. (2018) confirmed that the  $\beta$  Cyg A primary (Aa) is a typical red K giant, based on high-resolution spectroscopic measurements. These reveal that its surface gravity is consistent with having a mass of  $5 M_{\odot}$ . Thus the Scardia et al. (2007) orbit was falsified, and the possibility that  $\beta$  Cyg AB is a physical triple system cannot be excluded.

Later Roberts & Mason (2018) were able to present a formal orbit solution ( $P = 68.6 \pm 5.8$  yrs), thanks mainly to additional speckle observations accumulated by others. However, this later orbit led to a non-physical total mass of the system of  $85 M_{\odot}$ , and is in stark contrast to the *Gaia* DR2 proper motion of  $\beta$  Cyg A (see Bastian & Anton (2018)). Most recently a new orbit solution has been published by Scardia et al. (2019) using new speckle data, with a period of 120 years. However, its uncertainties are such that even this one must still be considered a preliminary solution (Scardia, private communication).

After a presentation of the data in Section 2, in Section 3 we present a new careful spectroscopic analysis and derive physical parameters of the two stars of  $\beta$  Cyg A as well as of  $\beta$  Cyg B, and estimate their ages under the assumption of a common distance. A first, well-constrained orbit solution for  $\beta$  Cyg Aa/Ab is presented in Section 4, based on both speckle and radial velocity measurements, with additional constraints from the HIPPARCOS and *Gaia* astrometry that allow us to constrain the total mass, distance and systemic velocities of the system. Using these, we evaluate the relationship between  $\beta$  Cyg A and B in Sections 5 and 6, assessing the possibility that they are a bound system with common origin, and we suggest that four stars may be additional stellar members belonging to it. Finally, we present the evidence that  $\beta$  Cyg A contains an additional, unseen companion in Section 7, and end with a concluding discussion.

## 2 DATA

### 2.1 Radial velocity data

For the purpose of orbit reconstruction the most useful of the early observing programs is that of Lick Observatory, which culminated in a large catalogue of radial velocities (Campbell 1928). This compilation contains 29 observations of  $\beta$  Cyg A taken over a period of 28 years using two different spectrographic instruments mounted on the 36 inch refractor on Mt. Hamilton. Uncertainties on the individual measurements are not provided, so we have assigned to these a provisional (and admittedly optimistic) uncertainty of  $1 \text{ km s}^{-1}$ , though we expect that the observations from the later New Mills instrument are of better quality than those from its predecessor. In any case, the uncertainties for these and the following radial velocity datasets will be checked against the standard deviation of the normalized residuals with respect to a satisfactory orbit solution.

In the same time period as covered by the Lick Observatory program only a few observations from other observatories can be found, but over much smaller temporal baselines, and usually of lower quality. Later radial velocity catalogues list  $\beta$  Cyg A as a single entry, giving its mean radial velocity (RV) derived from the compilation of the available observations from multiple observing programs over many years (e.g. Wilson (1953)), so are not useful for orbit determination.

Following the Lick Observatory program there is a long period of more than 40 years during which RV measurements of  $\beta$  Cyg A are few and of very limited quality, though it is worth mentioning the compilation of Hendry (1981), who also contributed her own observations taken over a twelve year period. From this heterogeneous compilation we take only the observations made by E. Hendry herself, made with the Northwestern University 1.1m LARC telescope<sup>1</sup>. We converted her quoted *probable errors* to standard errors assuming that these were estimated from the standard error  $\sigma$ , i.e.  $\gamma = 0.6745\sigma$ . Though this data set is of inferior quality, it partially fills the large gap between Lick and modern instruments and, as discussed later, its inclusion improves the quality of resulting orbit solutions.

Fortunately, modern RV surveys would soon begin to observe  $\beta$  Cyg A with a regular cadence and with superior instrumentation than was previously available. In particular, here we present two new datasets: 14 individual RV measurements made with CORAVEL on the 1 m Swiss telescope at the Haute-Provence Observatory made between 1981 and 1998, kindly provided by B. Famaey (private communication), followed by 12 recent RV measurements based on a series of high-resolution ( $R \approx 20,000$ ) spectra with the HEROS spectrograph at the TIGRE telescope (Schmitt et al. 2014), using the methodology described in Mittag et al. (2018).

In summary, we have RV observations of the primary component  $\beta$  Cyg Aa spanning a baseline of more than 120 years, though with a large gap of about 40 years. The complete set of RV measurements used in this work is given in Table 1, and shown in Figure 5.

### 2.2 Speckle observations

For the speckle observations of  $\beta$  Cyg A we use the compilation in the Fourth Catalog of Interferometric Measurements of Binary Stars. (Hereafter FCIM, described in Hartkopf et al. (2001).)<sup>2</sup>, maintained by the USNO up to January of 2018. These observations span from 1976 to 2008. However, many of the observations for  $\beta$  Cyg A in the FCIM (listed under its WDS identifier 193043.29+275734.9) are missing uncertainties. We therefore assign uncertainties for all the Center for High Angular Resolution Astronomy (CHARA) speckle observations (those indicated with technique code "Sc") as prescribed by Table 3 of Hartkopf et al. (2000), while other missing uncertainties were recovered by consulting the original publications. Care was also taken to check that the uncertainties in the separation  $\rho$  were in consistent units, as the FCIM often reports the uncertainties as quoted in the original citations, where one sometimes find relative uncertainties (i.e.  $\delta\rho/\rho$ ) or the uncertainty in  $\rho$  in arcseconds. For convenience we list the FCIM observations, with the uncertainties just mentioned, in Table 2, where we also give additional information about the telescope and instrumentation used, in order to check for possible systematics between different telescope/instrument combinations. A literature search confirmed that additional speckle observations of  $\beta$  Cyg A have not been published since 2010, however Marco Scardia has kindly provided his most recent observation reported in Scardia et al. (2019), which is the last entry of Table 2. In summary, we note that most of the speckle observations come from one of two observing programs, the CHARA program covering the first 20 years, and those with the Pupil Interferometry Speckle camera and CORONAGRAPH (PISCO) instrument from 1995 and onwards.

<sup>1</sup> Identification of the observatory for each observation was confirmed with the assistance of E. Hendry, private communication.

<sup>2</sup> Currently hosted at <http://www.astro.gsu.edu/wds/int4.html>

**Table 1.** Radial velocity data and associated errors, in  $\text{km s}^{-1}$ . The epoch is in Julian Days and  $N_m$  is the number of independent measurements.

RV	$\sigma_{RV}$	epoch JD	$N_m$	Observatory/Instrument
-25.2	1	2414421.99	1	Lick/Original Mills
-26.2	1	2414482.79	1	Lick/Original Mills
-24.5	1	2414785.99	1	Lick/Original Mills
-25.3	1	2415239.76	1	Lick/Original Mills
-25.8	1	2415493.02	1	Lick/Original Mills
-24.55	1	2416687.84	2	Lick/New Mills
-25.15	1	2417747.86	2	Lick/New Mills
-26.1	1	2418906.76	2	Lick/New Mills
-25.5	1	2419033.58	1	Lick/New Mills
-24.5	1	2419168.93	2	Lick/New Mills
-24.2	1	2419353.6	2	Lick/New Mills
-23.2	1	2419570.77	2	Lick/New Mills
-23.2	1	2419571.97	2	Lick/New Mills
-23.8	1	2419869.01	1	Lick/New Mills
-24.4	1	2419890.92	1	Lick/New Mills
-23.5	1	2419891.92	1	Lick/New Mills
-24.1	1	2420196.06	1	Lick/New Mills
-23.4	1	2420197.08	1	Lick/New Mills
-22.5	1	2420201.05	1	Lick/New Mills
-22.8	1	2421288.06	1	Lick/New Mills
-23.6	1	2421289.07	1	Lick/New Mills
-22.0	1	2421360.92	2	Lick/New Mills
-23.05	1	2421388.98	2	Lick/New Mills
-22.1	1	2421783.91	1	Lick/New Mills
-21.6	1	2421876.63	1	Lick/New Mills
-22.4	1	2422962.66	1	Lick/New Mills
-22.4	1	2423203.99	1	Lick/New Mills
-23.2	1	2424689.98	1	Lick/New Mills
-22.8	1	2424706.00	1	Lick/New Mills
-23.4	2.7	2440128.072	1	NWU LARC
-22.4	1.9	2440131.092	1	NWU LARC
-23.1	1.6	2442243.181	1	NWU LARC
-23.2	3.9	2442616.183	1	NWU LARC
-23.5	2.2	2442972.123	1	NWU LARC
-24.3	4.2	2444046.247	1	NWU LARC
-22.7	4.7	2444364.271	1	NWU LARC
-25.2	4.7	2444403.239	1	NWU LARC
-23.55	0.29	2444859.341	1	HPO/CORAVEL
-23.62	0.28	2446586.511	1	HPO/CORAVEL
-23.84	0.28	2446959.624	1	HPO/CORAVEL
-23.47	0.29	2447082.249	1	HPO/CORAVEL
-23.67	0.33	2447472.267	1	HPO/CORAVEL
-24.03	0.33	2447649.66	1	HPO/CORAVEL
-24.29	0.33	2447831.327	1	HPO/CORAVEL
-23.97	0.35	2448292.759	1	HPO/CORAVEL
-24.26	0.35	2448849.339	1	HPO/CORAVEL
-24.25	0.34	2449179.518	1	HPO/CORAVEL
-24.64	0.29	2449569.489	1	HPO/CORAVEL
-24.61	0.35	2450443.21	1	HPO/CORAVEL
-24.60	0.34	2450702.346	1	HPO/CORAVEL
-24.72	0.36	2451005.529	1	HPO/CORAVEL
-25.07	0.17	2458391.554	1	TIGRE/HEROS
-25.29	0.15	2458446.559	1	TIGRE/HEROS
-25.71	0.12	2458527.019	1	TIGRE/HEROS
-25.78	0.12	2458528.014	1	TIGRE/HEROS
-25.73	0.12	2458529.013	1	TIGRE/HEROS
-25.79	0.12	2458577.969	1	TIGRE/HEROS
-25.70	0.11	2458612.927	1	TIGRE/HEROS
-25.63	0.12	2458624.889	1	TIGRE/HEROS
-25.71	0.11	2458671.814	1	TIGRE/HEROS
-25.06	0.16	2458717.658	1	TIGRE/HEROS
-25.10	0.16	2458748.564	1	TIGRE/HEROS
-25.16	0.17	2458770.596	1	TIGRE/HEROS

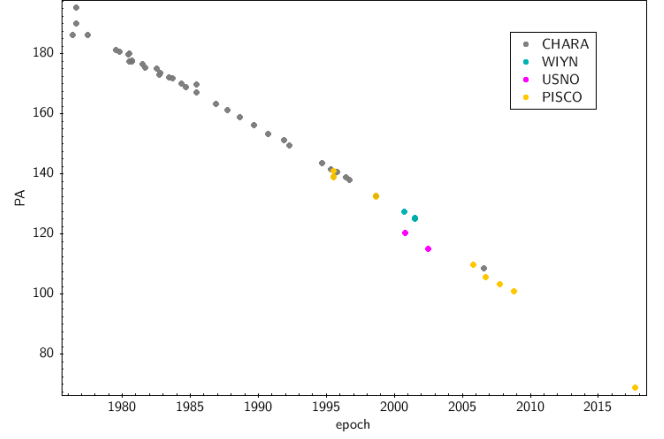


**Figure 1.** Position angle (PA) observations, in degrees, with respect to observing epoch.

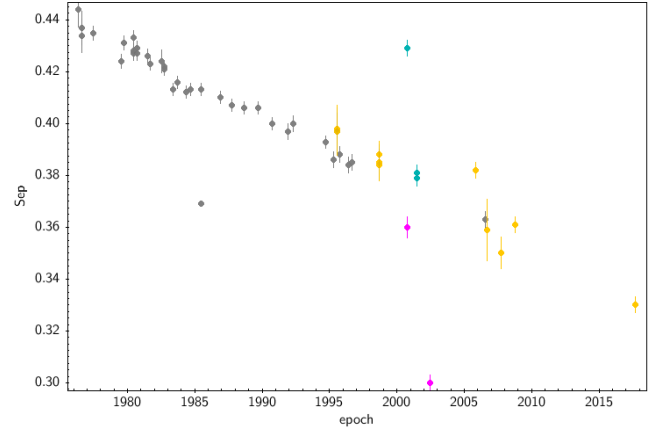


**Figure 2.** Separation, in arcseconds, with respect to observing epoch.

Taken together, the observed position angle (PA) measures show a smooth trend, with the exception of the two USNO observations which show a clear offset, as can be seen in Figure 1. Meanwhile, for the measured separations (Figure 2), we note that a number of the WIYN and USNO observations show large deviations from the otherwise smooth trend. For the purpose of orbit parameter estimation we therefore exclude the two USNO observations. In addition, we exclude one observation from the CHARA program: the single observation made with the 0.6 meter Lowell refractor (epoch JD1985.4729) with no estimated uncertainties.

### 2.3 Absolute astrometry

As mentioned in the Introduction, given its brightness, no reliable parallax for  $\beta$  Cyg A is available. However, for the purpose of estimating physical parameters in the following sections, we consider the hypothesis that  $\beta$  Cyg A is at the same distance as  $\beta$  Cyg B. For this star we find that the HIPPARCOS (Perryman et al. 1997; van Leeuwen 2007) and *Gaia* DR2 parallaxes are consistent, with a weighted mean of  $8.33 \pm 0.13$  mas, from which we adopt 120 pc as its nominal distance.

It is possible to use the  $\sim 25$  yr long temporal baseline provided

**Table 2.** Speckle data. Position angle (PA) and uncertainties are in degrees, separation ( $\rho$ ) is in arcseconds, the telescope and detector columns are derived from the source references, while the codes for these and technique code (last column) are taken directly from the FCIM.

epoch	PA	$\sigma_{PA}$	$\rho$	$\sigma_\rho/\rho$	Telescope	detector	reference code	Tech code
1976.3676	186.2	0.5	0.444	0.015	2.1 KPNO	phot	McA1982b	Sc
1976.6133	195.3	0.5	0.434	0.015	2.1 KPNO	phot	McA1982b	Sc
1976.6217	190.0	0.5	0.437	0.015	2.1 KPNO	phot	McA1982b	Sc
1977.4816	186.1	0.3	0.435	0.006	3.8 KPNO	phot	McA1979b	Sc
1979.5295	181.2	0.3	0.424	0.006	3.8 KPNO	phot	McA1982d	Sc
1979.7699	180.7	0.3	0.431	0.006	3.8 KPNO	phot	McA1982d	Sc
1980.4795	179.6	0.3	0.433	0.006	3.8 KPNO	phot	McA1983	Sc
1980.4823	180.0	0.3	0.428	0.006	3.8 KPNO	phot	McA1983	Sc
1980.4854	177.5	0.3	0.427	0.006	3.8 KPNO	phot	McA1983	Sc
1980.7173	177.4	0.3	0.427	0.006	3.8 KPNO	phot	McA1983	Sc
1980.7255	177.8	0.3	0.429	0.006	3.8 KPNO	phot	McA1983	Sc
1981.4735	176.4	0.3	0.426	0.006	3.8 KPNO	phot	McA1984a	Sc
1981.7003	175.3	0.3	0.423	0.006	3.8 KPNO	phot	McA1984a	Sc
1982.5277	175.1	0.5	0.424	0.010	1.8 Perk	oCDD	Fu1997	Sc
1982.7542	173.0	0.3	0.422	0.006	3.8 KPNO	oCDD	McA1987b	Sc
1982.7651	173.6	0.3	0.421	0.006	3.8 KPNO	oCDD	McA1987b	Sc
1983.4175	172.1	0.3	0.413	0.006	3.8 KPNO	nCCD	McA1987b	Sc
1983.7098	171.7	0.3	0.416	0.006	3.8 KPNO	nCCD	McA1987b	Sc
1984.3733	170.0	0.3	0.412	0.006	3.8 KPNO	nCCD	McA1987b	Sc
1984.7010	169.0	0.3	0.413	0.006	3.8 KPNO	nCCD	Hrt2000a	Sc
1985.4729	169.8		0.369		0.6 Low	nCCD	McA1987b	Sc
1985.4816	167.2	0.3	0.413	0.006	3.8 KPNO	nCCD	McA1987b	Sc
1986.8883	163.2	0.3	0.410	0.006	3.8 KPNO	nCCD	McA1989	Sc
1987.7618	161.2	0.3	0.407	0.006	3.8 KPNO	nCCD	McA1989	Sc
1988.6575	159.0	0.3	0.406	0.006	3.8 KPNO	nCCD	McA1990	Sc
1989.7112	156.3	0.3	0.406	0.006	3.8 KPNO	nCCD	Hrt2000a	Sc
1990.7434	153.3	0.3	0.400	0.006	3.8 KPNO	nCCD	Hrt1992b	Sc
1991.8959	151.2	0.3	0.397	0.008	3.8 KPNO	nCCD	Hrt1994	Sc
1992.3105	149.5	0.3	0.400	0.008	3.8 KPNO	nCCD	Hrt1994	Sc
1994.7080	143.6	0.3	0.393	0.006	3.8 KPNO	nCCD	Hrt2000a	Sc
1995.3141	141.5	0.4	0.386	0.008	2.5 MWO	nCCD	Hrt1997	Sc
1995.556	139.0	0.8	0.398	0.023	2.0 PdM	P-CAR	Pru2002b	S
1995.556	140.9	1.0	0.397	0.023	2.0 PdM	P-CAR	Pru2002b	S
1995.559	139.3	1.0	0.397	0.018	2.0 PdM	P-CAR	Pru2002b	S
1995.7620	140.7	0.4	0.388	0.008	2.5 MWO	nCCD	Hrt1997	Sc
1996.4227	139.0	0.4	0.384	0.008	2.5 MWO	nCCD	Hrt2000a	Sc
1996.6984	138.1	0.4	0.385	0.008	2.5 MWO	nCCD	Hrt2000a	Sc
1998.657	132.3	0.9	0.385	0.018	2.0 PdM	P-CCD	Pru2002b	S
1998.657	132.7	0.5	0.384	0.016	2.0 PdM	P-CCD	Pru2002b	S
1998.657	132.7	0.5	0.388	0.013	2.0 PdM	P-CCD	Pru2002b	S
2000.7614	127.3	1.0	0.429	0.007	3.5 WIYN	CCD	Hor2002a	S
2000.7854	120.3	0.5	0.36	0.011	0.7 USNO	iCCD	WSI2001b	Su
2001.4930	125.3	0.6	0.379	0.008	3.5 WIYN	RYTSI	Hor2008	S
2001.4930	125.0	0.6	0.381	0.008	3.5 WIYN	RYTSI	Hor2008	S
2002.473	115.1	0.6	0.30	0.010	0.7 USNO	iCCD	WSI2004a	Su
2005.820	109.7	0.3	0.382	0.008	1.0 Zeiss	PISCO	Sca2008a	S
2006.5723	108.6	0.4	0.363	0.008	2.5 MWO	nCCD	Hrt2009	Sc
2006.721	105.5	1.3	0.359	0.033	1.0 Zeiss	PISCO	Sca2009a	S
2007.770	103.3	0.4	0.350	0.017	1.0 Zeiss	PISCO	Sca2010c	S
2008.802	100.8	1.4	0.361	0.008	1.0 Zeiss	PISCO	Pru2010	S
2017.6873	68.9	0.3	0.330	0.009	1.0 CERGA	PISCO	Sca2019	S

by the *HIPPARCOS* and *Gaia* position measurements, as well as their absolute proper motions, to trace the orbital motion of  $\beta$  Cyg Aa due to  $\beta$  Cyg Ac. This is a desirable addition, as *HIPPARCOS* and *Gaia* astrometry provides constraints complementary to those of the RV and speckle imaging astrometry, allowing in particular to directly infer the mass ratio. Evidence of orbital motion effects due to a perturbing companion is obtained by measuring proper motion changes between appropriately cross-calibrated catalogues. This approach is usually referred to as 'proper motion difference', 'astrometric acceleration',

or 'proper motion anomaly' technique, in short  $\Delta\mu$ . Past applications of the methodology include catalogues of  $\Delta\mu$  binaries (Wielen et al. 2000; Makarov & Kaplan 2005; Tokovinin et al. 2012) produced by comparison of catalogues (e.g., *HIPPARCOS*) including short-term proper motions (that capture the reflex orbital motion of the primary) with those (e.g., Tycho-2) based on long-term observations of star positions (for which the long-term proper motion will be closer to the true center-of-mass motion of the system). More recently, the  $\Delta\mu$  technique has been applied to detect (or place upper limits on) stel-



**Table 3.** Astrometry data with uncertainties. The third column reports the catalogue origin of the proper motions, with T = Tycho-2, H = revised HIPPARCOS, G = *Gaia* DR2, H' and G' = cross-calibrated values from the Brandt (2018) catalogue, B = proper motions from H' and G' positions. Units are all mas yr<sup>-1</sup>.

object	sourceid	catalogue	$\mu_\alpha$	$\sigma_{\mu_\alpha}$	$\mu_\delta$	$\sigma_{\mu_\delta}$	$\varpi$	$\sigma_\varpi$
$\beta$ Cyg A	2133-2964-1	T	-1.5	0.3	-1.4	0.3		
	95947	H	-7.17	0.25	-6.15	0.33	7.51	0.33
	2026116260302988160	G	6.127	1.164	-15.488	1.091	9.95	0.60
		H'	-7.06	0.43	-5.77	0.53		
		G'	6.126	2.104	-15.488	1.972		
		B	-2.038	0.040	-10.018	0.042		
$\beta$ Cyg B	2133-2963-1	T	-0.5	1.2	-1.9	1.1		
	95951	H	-1.9	0.19	-1.02	0.27	8.16	0.25
	2026113339752723456	G	-0.990	0.261	-0.541	0.275	8.38	0.16
		H'	-1.880	0.412	-0.805	0.508		
		G'	-0.990	0.471	-0.541	0.497		
		B	-1.044	0.016	-1.442	0.019		

lar and substellar companions using the HIPPARCOS and *Gaia* DR2 catalogues (Calissendorff & Janson 2018; Snellen & Brown 2018; Kervella et al. 2019; Brandt et al. 2019; Dupuy et al. 2019; Feng et al. 2019; Grandjean et al. 2019; Kervella et al. 2020; Damasso et al. 2020; De Rosa et al. 2020; Xuan & Wyatt 2020). In such cases, the long-term proper motion vector (assumed to be describing the barycenter tangential velocity) is determined from the difference in astrometric position between the two catalogues divided by the corresponding  $\sim 25$ -yr time baseline. By subtracting this long-term proper motion from the quasi-instantaneous proper motions of the two catalogues one obtains a pair of  $\Delta\mu$  values assumed to be entirely describing the projected velocity of the photocenter around the barycentre at the HIPPARCOS and *Gaia* DR2 epochs.

To include a time series of absolute astrometry for  $\beta$  Cyg Aa in our analysis, we take the cross-calibrated HIPPARCOS/*Gaia* DR2 proper motion values and the scaled HIPPARCOS-*Gaia* positional difference from the Brandt (2018, 2019) catalogue of astrometric accelerations<sup>3</sup>. However, Brandt (2018) warns against blind use of the  $\Delta\mu$  technique in cases of accelerating stars that are binaries with modest brightness ratios and/or stars with particularly large errors in the astrometry. This is indeed the case for  $\beta$  Cyg Aa: due to its brightness, it is highly saturated in *Gaia* data, and  $\beta$  Cyg Ac is only 2.2 mag fainter at V band (see Table 5). Furthermore, it is questionable whether the scaled HIPPARCOS-*Gaia* positional difference, spanning only  $\sim 20\%$  of the orbital phase, can really be considered as a close representation of the barycentre tangential velocity. In our analysis, we then decide to utilize the three proper motions separately<sup>4</sup>. We report in Table 3 the positions and proper motions of both  $\beta$  Cyg A and B from HIPPARCOS, *Gaia* and Tycho-2, as well as  $\beta$  Cyg A's cross-calibrated HIPPARCOS and *Gaia* proper motions and the corresponding scaled position difference as derived by Brandt (2018, 2019). These values

will be utilized in our final orbit solution of the  $\beta$  Cyg A system, and in the discussion of its relation to  $\beta$  Cyg B.

### 3 PHYSICAL PARAMETERS FROM SPECTROSCOPY AND EVOLUTION MODELS

We present in Figures A5 and A6 the high resolution ( $R \approx 20,000$ ) spectrum obtained with the TIGRE telescope. The spectrum contains contributions from both stars  $\beta$  Cyg Aa and  $\beta$  Cyg Ac. Blueward of 4000 Angstroms the Balmer series of the blue main-sequence companion  $\beta$  Cyg Ac can be clearly identified (Fig. A5). The rest of the spectrum is dominated by the various lines of the giant star  $\beta$  Cyg Aa, the Ca II triplet being clearly seen redward of 8475 Angstroms (last row of Fig. A6).

#### 3.1 Albireo Aa, the red supergiant primary

To improve our earlier spectroscopic determination of the physical parameters (see Jack et al. (2018)), we added all observed spectra to obtain a single spectrum with a very high S/N. Before this step, all spectra were corrected individually for their respective radial velocity against the laboratory wavelength scale. In this improved analysis we now also used some unblended lines recorded in the blue channel of HEROS.

To avoid confusion with the spectral contributions from the very near component Ac, which falls into the 3 arcseconds spanning aperture of the optical fibre feeding HEROS, and from line blanketing too strong to define a continuum, we restricted this work to lines redwards of 4900 Å. In the red channel of the HEROS spectrograph we also excluded all regions which are affected by telluric line absorption.

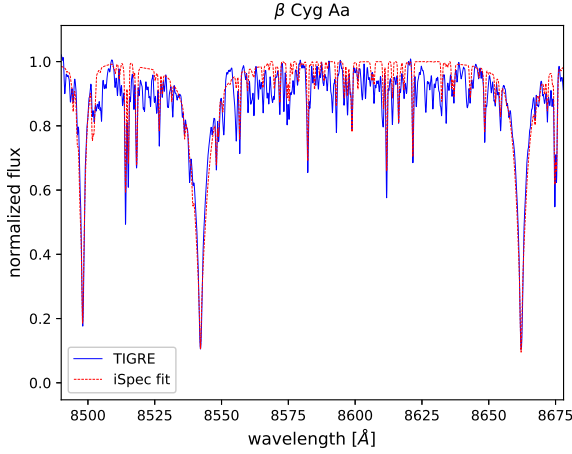
The parameter-fitting procedure was carried out with the spectral analysis tool-kit iSpec (Blanco-Cuaresma et al. 2014) in its most recent version (v2019.03.02), described by Blanco-Cuaresma (2019). In that work, the creator of iSpec recommends the use of a list of specific lines, which are matching the solar spectrum very well for the known physical parameters of the Sun. However, using these lines in our work, we found that the suggested best-fit parameters depend on the choice of their initial values (which they should not), especially when several parameters are optimized in the same run. Total error sums  $\chi^2$  of such competing parameter-fits differ very little. We suspect that this is the effect of working here in a regime of lower temperature and gravity, as compared to the Sun. Thus, we here did not use that suggested line list, but instead we started with

<sup>3</sup> Brandt (2018, 2019) employs a linear combination of the original (Perryman et al. 1997) and new (van Leeuwen 2007) reductions of the HIPPARCOS data to estimate star positions, as a way to mitigate the systematics associated with each of the catalogues considered individually. We actually adopt the version of the catalogue published in Brandt (2019), which corrects an error in the calculation of the perspective acceleration in R.A. and effectively supersedes the original catalogue presented in Brandt (2018).

<sup>4</sup> Following Lindegren (2020a,b), when calculating the HIPPARCOS - *Gaia* position differences divided by the epoch difference we subtract the (small) cross-calibration corrections applied by Brandt (2018, 2019) in order to place them on the ICRS.

**Table 4.** Stellar parameters of  $\beta$  Cyg Aa as determined by spectroscopic analysis

Parameter	Value
$T_{\text{eff}}$	$4382.7 \pm 2.1$ K
$\log g$	$0.93 \pm 0.01$
$[M/H]$	0.02
$[\alpha/Fe]$	0.08
$v_{\text{mic}}$	$1.57 \text{ km s}^{-1}$
$v_{\text{mac}}$	$5.22 \text{ km s}^{-1}$
$v \sin i$	$8.34 \pm 0.4 \text{ km s}^{-1}$

**Figure 3.** The observed TIGRE spectrum with the iSpec fit in the region of the Ca triplet.

the GES line list (Gilmore et al. 2012; Randich et al. 2013), and in the wavelength range from 4900 to 8800 Å we then selected those spectral segments without telluric contamination.

As suggested by Blanco-Cuaresma (2019), we used the iSpec parameter-fitting option, which is based on the SPECTRUM code (Gray & Corbally 1994), and as solar abundances we chose the ones of Grevesse et al. (2007). The atmospheric model spectra used by us in iSpec for the best-fit comparison are of the MARCS code (Gustafsson et al. 2008). To obtain a reasonable value for the rotation velocity, we fixed the micro and macro turbulence velocities by the empirical relation offered now by iSpec in its newest version.

The results of this spectroscopic stellar parameter determination for  $\beta$  Cyg Aa by iSpec are listed in Table 4. Most importantly, the effective temperature (essentially unchanged from Jack et al. (2018)) of  $T_{\text{eff}} = 4382.7 \pm 2.1$  K will be used for the evolution modelling to obtain mass and age of component Aa in the following section. We note that the quoted uncertainty of  $T_{\text{eff}}$  is the internal error (of the fitting process), and that the total uncertainty is more like 60 K (see Schröder et al. (2020a)). The conclusion of Jack et al. (2018), that  $\beta$  Cyg Aa is a normal giant star, below is confirmed and substantiated.

There are some small differences to our previous results (Jack et al. (2018)). For example, the spectroscopic surface gravity here is slightly higher. This actually improves consistency with the gravity ( $\log g = 1.57$ ), which we compute from the mass of  $5.2M_{\odot}$  of the best-fit evolutionary model for Aa (see next section), and the radius of  $62R_{\odot}$  resulting from the luminosity and effective temperature. In

**Table 5.** Physical parameters of the Albireo components

component	Aa	Ac	B
$V$	$3.21 \pm 0.04$	5.85	$5.11 \pm 0.02$
$B$	$4.45 \pm 0.04$		$5.01 \pm 0.02$
$B - V$	$1.25 \pm 0.05$		$-0.10 \pm 0.03$
BC	$-0.80 \pm 0.10$	$-0.40 \pm 0.10$	$-0.85 \pm 0.10$
$M_{\text{Bol}}$	$-3.01 \pm 0.13$	+0.05 :	$-1.16 \pm 0.12$
$\log L/L_{\odot}$	$3.10 \pm 0.05$	$1.9 \pm 0.1$ :	$2.36 \pm 0.05$
$\log T/K$	$3.64 \pm 0.02$	$4.0 \pm 0.05$	$4.121 \pm 0.02$
$M/M_{\odot}$	$5.2 \pm 0.1$	$2.7 \pm 0.1$	$3.7 \pm 0.05$

a work on the Hyades K giants (Schröder et al. 2020b), we have already noted this same tendency. i.e. that iSpec best-fit gravities turn out about 0.5 dex lower than the computational value. However, cross-talk with effective temperature values is still small on this scale: Setting the gravity up to such a larger value, the value suggested by iSpec for  $T_{\text{eff}}$  changes by less than 2%.

As a new spectroscopic parameter, the  $\alpha$  enhancement of Albireo Aa was obtained by us here as +0.08. And with the values for the micro and macro-turbulence taken from empirical relations, we determined a notable rotational velocity for the giant of  $v \sin i = 8.34 \pm 0.4 \text{ km s}^{-1}$ . It is worth mentioning that the errors given in Table 4 are the errors of the fitting procedure and do not include any systematic errors, which we attempt to estimate and add in the following.

### 3.1.1 Photometric properties

In Table 5 we list the photometric properties of the primary star Aa which result from subtraction of the small contributions of Ac (see below) to the B and V magnitudes given by SIMBAD for the composite light of Albireo A. They are followed by the respective luminosity. Here we are using as the distance of  $\beta$  Cyg A that of  $\beta$  Cyg B (120pc), for the reasons discussed in Section 2.

As bolometric correction for the supergiant primary Aa we use  $BC = -0.80$ , as taken from Flower (1996, see Fig 4 therein), which corresponds to the colour ( $B - V = 1.25$ ) and the effective temperature of Aa derived above. Apart from the debated parallax and true distance to  $\beta$  Cyg A the bolometric correction presents the other larger uncertainty in the luminosity of Aa, since BC is changing steeply around the effective temperature of this red supergiant.

### 3.2 The very close secondary Ac

Like Albireo B, the close companion Ac is a hot main-sequence star. Since its separation from the bright primary Aa is less than an arcsecond in the sky, Ac is in the seeing-related glare of Aa. Consequently, the assessment of the physical parameters of Ac is severely affected. This being a physical binary as described above, and so the distance of Ac without doubt should be same as the one adopted above for Aa (120 pc). The CCDM entry of Ac suggests  $V=5.5$  but without any reference. A work dedicated to close binary components by ten Brummelaar et al. (2000), using speckle differential photometry on the venerable 100 inch Mt. Wilson reflector, measured a visual magnitude difference between Aa and Ac of 2.64 mag, bringing Ac to a more credible  $V=5.85$  mag. In addition, the spectral type of B9.5V would suggest a B-V value of close to 0.0, and an effective temperature of close to 10,000 K, but that we must regard as uncertain.

IUE took a low-resolution SWP spectrum of Albireo. Using the larger (10 arcseconds wide) slit, in which the small displacement of Ac against Aa is irrelevant. The giant component Aa already being very weak in the far UV, this spectrum seemed promising for getting additional information on effective Temperature and luminosity of Ac. However, comparing its SED (spectral energy distribution) with PHOENIX models, the best-matching  $T_{\text{eff}}$  remains ambiguous. While the very notable flux beyond Ly-alpha, i.e. shortward of 121nm, suggests Ac to be hotter than 11,000 K, the long wavelength end of the SED (170-220 nm) has a slope, which is better consistent with spectra of 10,200 K models. Within this uncertainty in  $T_{\text{eff}}$ , which quadruples into the respective luminosity estimate, we can only say that the IUE SWP fluxes are consistent with a 5.85 magnitude A0-B9 main sequence star at the distance of Albireo within a factor of 2. The synthetic spectra used here are of non-LTE PHOENIX models with  $\log g = 5.0$  and solar metallicity, obtained from the PHOENIX model library, made publically available by the University of Göttingen and described by [Husser et al. \(2013\)](#). To match the IUE SWP low dispersion, we reduced the resolution of the synthetic spectra adequately with iSpec.

### 3.3 Albireo B, the far hot companion

Albireo B is separated from Aa by 34 arcseconds, and it is a bright ( $m_V = 5.11$  mag) star in its own right. Not surprisingly then, it has been studied well in the past. We adopt  $T_{\text{eff}}=13,200$  K according to [Levenhagen & Leister \(2004\)](#) and consistent with the spectral type of B8V. With a BC of  $-0.85$  (according to [Flower \(1996\)](#), see Fig. 4 therein), and a distance of 120 pc, we then obtain a luminosity of  $229 L_{\odot}$  ( $\log L/L_{\odot} = 2.36$ , see Table 5).

Again, as with Aa, the bolometric correction here seems to be the other main source of uncertainty, since Albireo B, too, lies in a temperature range, where BC changes steeply.

### 3.4 Masses by evolution modelling - same age?

Matching the physical quantities of each of the Albireo component stars with an evolution track in the HRD (i.e.  $\log T_{\text{eff}}$  and  $\log L/L_{\odot}$ ) reveals their masses and ages. For this work, we are using the well-tested evolution models of the Eggleton code (see [Schröder et al. \(1997\)](#) and [Pols et al. \(1997\)](#)), where the amount of "overshooting" (in better words: extra mixing) and the mixing length itself was carefully calibrated against eclipsing binaries and stellar cluster isochrones in the mass-range relevant for this study.

If Albireo was once formed as a hierarchical triple, or may even still be one (see below), then all three stars should be matched with models of the same age. A star on the main sequence, like the companions Ac and B, changes its HRD position only slowly, and so its match is less critical. On the contrary, giant star evolution is fast and therefore a sensitive indicator of age.

For the primary, Albireo Aa, we find a very good match with an evolution track of a mass of  $5.2 M_{\odot}$ , as just starting its central He-burning (see Fig. 4). Since the abundances of Albireo are not much different from solar, we computed that track (and all others shown here) for a metallicity of  $Z=0.02$ .

The early central helium burning is about the slowest phase in the evolution of a red giant with a few solar masses. By contrast, a star with the mass of Albireo Aa passes its shell-burning phases quite fast. Therefore, the onset of central helium-burning has the largest probability, compared with alternative evolutionary tracks, which would — within the uncertainties — match the present HRD

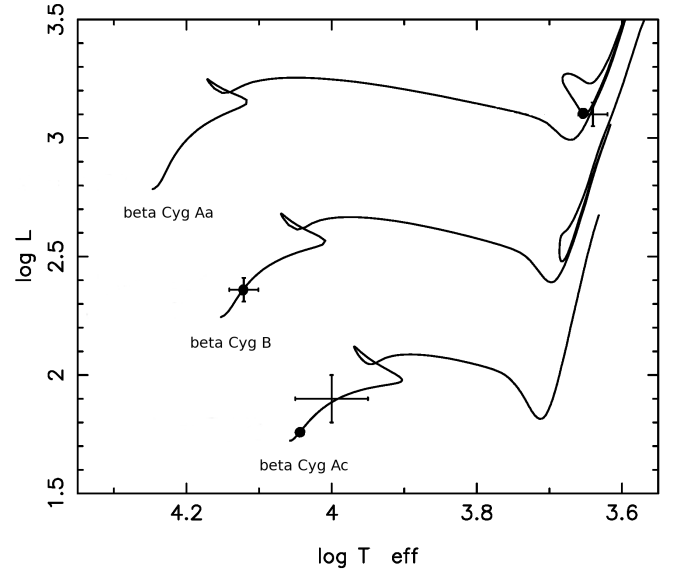


**Figure 4.** Evolutionary tracks with the suggested masses of the three Albireo components, of  $5.2 M_{\odot}$  for the primary (Aa),  $3.7 M_{\odot}$  for the wide companion Albireo B, and  $2.7 M_{\odot}$  for the close secondary (Ac). (Luminosity is with respect to solar, and the effective temperature is in Kelvin.) The age of 99 Myrs is best defined by the primary, which is starting central helium burning, and Albireo B matches that age mark very well, Ac still within its larger error bars. The physical parameters and their estimated uncertainties are as listed in Table 5.

location. At the same time this solution points to a well-defined age for the Albireo primary, of 99 Myrs.

Within their uncertainties discussed above (and see Table 5), the two companions are matched well with evolution tracks of  $3.7 M_{\odot}$  for Albireo B and  $2.7 M_{\odot}$  for the close secondary Ac, see Fig. 4, while coinciding with the age of Aa. We would like to emphasize the perfect age match of the distant companion Albireo B with the primary Aa. This may not prove a common origin as a hierarchical triple, but it supports this idea to be, at the least, very likely.

In the case of Ac, this coincidence looks near marginal, though, as if Ac was already more evolved, that is: having a larger content of Helium than the age of Aa and an undisturbed evolution as a single star would suggest. But by means of the orbit there can be no doubt, that Albireo Aa/Ac is a bound system, which was formed together. To resolve this issue, as well as the larger system mass and mass ratio demanded by astrometry, when compared to the here given astrophysical account of the visible mass, see further suggestions on the nature of Ac in our discussion below.

## 4 ORBIT SOLUTIONS

### 4.1 Preliminary RV orbital solutions

As a first step in the derivation of an updated orbital solution for the  $\beta$  Cyg A system, we analysed all the RV data available (described in Section 2.1) with tools commonly used in the analysis of RV extrasolar planets (e.g. [Pinamonti et al. 2018](#)). This is a particularly interesting case for such an analysis, since Albireo has one of the longest baselines of RV data ever collected.

The model adopted to describe the radial velocity time series is

**Table 6.** Priors and best-fit results for the `emcee` analysis of the combined RV time series of  $\beta$  Cyg Aa, for a Keplerian model of the Aa/Ac system.

parameter	Prior	Short period Best-fit value	Prior	Long period Best-fit value
$\gamma_{\text{sys}}$ [km s $^{-1}$ ]	$\mathcal{U}(-30, 20)$	$-24.33^{+0.10}_{-0.13}$	$\mathcal{U}(-30, 20)$	$-23.59^{+0.21}_{-0.20}$
$K$ [km s $^{-1}$ ]	$\mathcal{U}(0, 4)$	$1.40^{+0.20}_{-0.24}$	$\mathcal{U}(0, 4)$	$1.84^{+0.30}_{-0.23}$
$P$ [years]	$\mathcal{U}(40, 100)$	$55.7^{+2.0}_{-1.1}$	$\mathcal{U}(105, 150)$	$120.5^{+15.3}_{-7.4}$
$T_0$ [BJD-2410000]	$\mathcal{U}(0, 50000)$	$18000^{+1400}_{-1500}$	$\mathcal{U}(0, 50000)$	$36200^{+2200}_{-1900}$
$\sqrt{e} \cdot \cos \omega$	$\mathcal{U}(-1.0, 1.0)$	$0.11^{+0.16}_{-0.22}$	$\mathcal{U}(-1.0, 1.0)$	$-0.20^{+0.19}_{-0.14}$
$\sqrt{e} \cdot \sin \omega$	$\mathcal{U}(-1.0, 1.0)$	$-0.69^{+0.13}_{-0.09}$	$\mathcal{U}(-1.0, 1.0)$	$-0.58^{+0.15}_{-0.14}$
<i>Derived quantities</i>				
$e$		$0.52^{+0.13}_{-0.14}$		$0.40^{+0.20}_{-0.15}$
$\omega$ [rad]		$-1.40^{+0.26}_{-0.32}$		$-1.89^{+0.30}_{-0.24}$

the following:

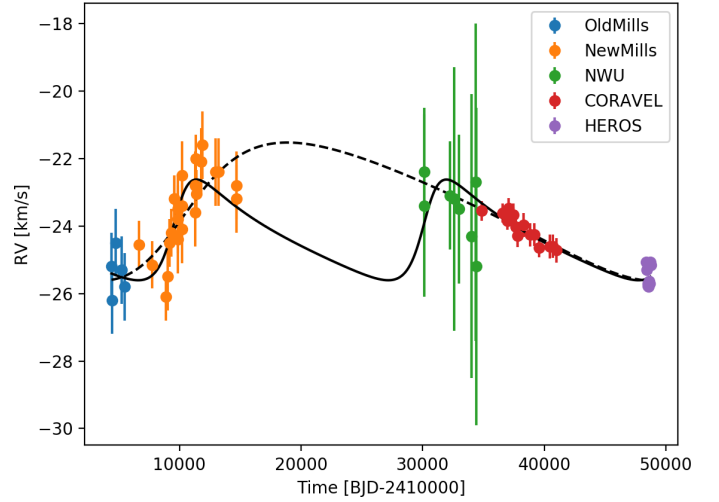
$$RV_{\text{mod}} = \gamma_{\text{sys}} + K \cos(\nu(t, e, T_0, P) + \omega) + e \cos(\omega), \quad (1)$$

where  $\gamma_{\text{sys}}$  is the systemic radial velocity of the system,  $K$  is the semi-amplitude of the Keplerian signal, and the true anomaly  $\nu$  is a function of time  $t$ , time of the inferior conjunction  $T_0$ , orbital period  $P$ , eccentricity  $e$  and argument of periastron  $\omega$ . We choose not to consider different RV offset values for the different instruments, since most time series have very short timespans compared to the expected orbital period of the binary, and thus the additional degree of freedom given by the offset would almost void the contribution of the short-baseline datasets to the fit.<sup>5</sup> Moreover, instead of fitting separately the eccentricity  $e$  and argument of periastron  $\omega$ , we define the auxiliary parameters  $e \cdot \cos(\omega)$  and  $e \cdot \sin(\omega)$  in order to reduce the covariance between the fitted parameters.

The model described in Eq. 1 is fitted via MCMC analysis, performed with the publicly available `emcee` algorithm (Foreman-Mackey et al. 2013). We used 100 random walkers to sample the parameter space. The posterior distributions were derived after applying a burn-in phase of 3000 steps, as explained in Eastman et al. (2013, and references therein). To evaluate the convergence of the different MCMC analyses, we calculated the integrated correlation time for each of the parameters, and stopped the code after a number of steps equal to 200 times the largest autocorrelation times of all the parameters (Foreman-Mackey et al. 2013).

We tested different initial configurations for the `emcee` code as well as different priors for the orbital parameters, in order to test the different orbital solutions from the literature (Hartkopf 1999; Scardia et al. 2007). Long-period and short-period solutions were treated separately, since the `emcee` code is susceptible to multi-modal probability distributions (Foreman-Mackey et al. 2013). We found the best-fit solutions to be the two obtained with the priors listed in Table 6, and shown in Fig. 5, respectively one for a short-period orbit, and one for a long-period orbit. The best fit results are described by the median of the distribution and the asymmetric error bars obtained from the 16th-84th percentiles.

As shown in Fig. 5, the presented solutions follow closely the RV data of the binary system. Moreover, we compared the rms of the RV residuals, after the subtraction of  $\gamma_{\text{sys}}$  and Keplerian signal, with the mean uncertainty  $\langle \sigma_i \rangle$  of each dataset  $i$ : we obtained  $\text{rms}/\langle \sigma_i \rangle < 0.9$  for all datasets. This is further evidence of the goodness of the two fits, since no excess noise is present in the RV residuals. **However**, it is

**Figure 5.** Short- and long-period orbital solutions for the Aa-Ac system compared with the five radial velocity time series considered in the analysis. Color of the data points notes the telescope/instrument used, as noted in Table 1, where LOM = Lick/Original Mills, LNM = Lick/New Mills, NWU = NWU LARC, HPO = HPO/CORAVEL, KIT = Kitt Peak, and HEROS = TIGRE/HEROS.

impossible to distinguish between long- and short-period solutions: adopting the Bayesian information criterion (BIC, Schwarz 1978) we obtained  $\Delta\text{BIC} = 0.17$  between the two models, which corresponds to no statistical evidence in favour of one or the other. This is an indication of the fact that the RV data alone, due to the short baseline compared to the orbital period, and the sparse sampling, cannot give a precise measurement of the orbital parameters of the  $\beta$  Cyg A system on their own.

## 4.2 Orbital solution from RVs and relative astrometry

A Bayesian analysis of the combined RV and speckle observations was performed using a differential evolution Markov chain Monte Carlo (DE-MCMC) method (Ter Braak 2006; Eastman et al. 2013). We took advantage of the six ( $A$ ,  $B$ ,  $C$ ,  $F$ ,  $G$ ,  $H$ ) Thiele-Innes constants representation (e.g. Binnendijk (1960); Wright & Howard (2009)) to partially linearize the problem in both astrometry and RV. Within this dimensionality reduction scheme, only three non-linear orbital parameters must be effectively explored using the DE-MCMC algorithm (e.g., Casertano et al. (2008); Wright & Howard (2009); Mendez et al. (2017)), namely  $P$ ,  $T_0$ , and  $e$ . At each step of the DE-MCMC analysis, the resulting linear system of equations is solved in terms of the Thiele-Innes constants using simple matrix algebra, singular value decomposition and back-substitution being the method of choice. Standard formulae are then applied (e.g., Casertano et al. (2008); Wright & Howard (2009); Mendez et al. (2017)) to convert from the Thiele-Innes constants back to the remaining Campbell elements (semi-major axis  $a$ , inclination angle  $i$ , argument of periastron  $\omega$ , and longitude of the ascending node  $\Omega$ ),  $K$ , and  $\gamma_{\text{sys}}$ . The speckle imaging astrometry and RV time series were modelled using the

<sup>5</sup> We explored the addition of instrumental offsets to the RV-only model, but the test fit (not shown), resulted in uncertainties almost as large as the priors.



following likelihood function:

$$\ln \mathcal{L} = -\frac{1}{2} \left( \sum_{i=1}^{N_{RV}} \left( \frac{RV_i^{(obs)} - RV_i^{(model)}}{\sigma_{RV,i}} \right)^2 + \sum_{j=1}^{N_{astr}} \left( \frac{X_j^{(obs)} - X_j^{(model)}}{\sigma_{X,j}} \right)^2 + \sum_{j=1}^{N_{astr}} \left( \frac{Y_j^{(obs)} - Y_j^{(model)}}{\sigma_{Y,j}} \right)^2 \right) \quad (2)$$

where  $N_{RV}$ , and  $N_{astr}$  are the number of RV and astrometric measurements, respectively, and  $\sigma$  the corresponding measurement errors. At this stage, we did not consider offsets between datasets obtained by different instruments. The DE-MCMC analysis was carried out with a number of chains equal to twice the number of free parameters, and it was stopped after it reached convergence and good mixing of the chains based on the Gelman-Rubin statistics (e.g., Ford (2006)). After removing 20% of burn-in steps, the medians of the posterior distributions and their  $\pm 34.13\%$  intervals were evaluated and were taken as the final parameters and associated  $1\sigma$  uncertainties. The final results are reported in Table 7. Overall, the combination of RV and speckle imaging astrometry allows to constrain rather robustly the orbital configuration of the Albireo Aa,c components. As a cross-check, the  $\omega$  value derived from the Thiele-Innes representation for the RV model (describing the primary orbital motion) differs exactly by 180 deg from the one obtained from the astrometry model (that describes the secondary orbit). We also explored solutions in the neighbourhood of the short ( $\sim 55$  yr) and long ( $\sim 210$  yr) period orbits derived with RV-only data in Sect. 4.1 and by Scardia et al. (2007), respectively, but these attempts returned lower likelihoods, and thus disfavoured solutions with respect to the one reported in Table 7.

Finally, assuming a distance of 120 pc (i.e. a parallax of 0.00833 arcsec), and given the values of  $a$  (in arcsec),  $P$  (in yr),  $e$ ,  $i$ , and  $K$  (in  $\text{km s}^{-1}$ ) from 7, we can derive the mass ratio  $q = M_{Ac}/M_{Aa}$  from e.g. Eq. 12 in Pourbaix & Jorissen (2000):

$$\frac{1}{1 + 1/q} = 0.0335729138 \frac{PK\sqrt{1 - e^2}\varpi}{a \sin i}. \quad (3)$$

We obtain  $q = 0.53^{+0.13}_{-0.09}$ . At the same distance, the total system mass can be inferred to be  $7.55^{+0.57}_{-0.56}$  solar masses.

### 4.3 Final orbit solution

As discussed in Section 2.3, the inclusion of the available information on the orbital motion of  $\beta$  Cyg Aa coming from absolute astrometry allows one to obtain an estimate of the mass ratio in addition to the complete set of orbital elements. For the reasons outlined in Section 2.3, we decide to proceed using the three individual values of absolute proper motion rather than two proper motion differences. As a consequence, we need to solve not only for the mass ratio ( $q$ ) but also for the two components of the proper motion of the barycentre of the system ( $\mu_{RA}^b$ ,  $\mu_{DEC}^b$ ). The DE-MCMC orbital fit analysis is then carried out on the time-series of absolute proper motions so defined, the RV and speckle imaging datasets, adding  $q$ ,  $\mu_{RA}^b$ , and  $\mu_{DEC}^b$  as new model parameters effectively explored using

**Table 7.** Priors and best-fit results for the DE-MCMC analysis of the combined RV + speckle imaging time series.

Parameter	Prior	Best-fit value
$P$ [yr]	$\mathcal{U}(100,150)$	$125.52^{+3.77}_{-2.96}$
$T_0$ [yr]	$\mathcal{U}(2000.0,2050.0)$	$2024.94^{+1.01}_{-1.30}$
$e$	$\mathcal{U}(0.0,0.99)$	$0.21^{+0.02}_{-0.01}$
<i>Derived quantities:</i>		
$a$ [arcsec]		$0.409^{+0.008}_{-0.006}$
$i$ [deg]		$24.53^{+2.10}_{-2.38}$
$\Omega$ [deg]		$88.96^{+5.65}_{-4.12}$
$\omega$ [deg]		$53.05^{+1.92}_{-2.36}$
$\gamma_{\text{sys}}$ [ $\text{km s}^{-1}$ ]		$-23.71^{+0.08}_{-0.10}$
$K$ [ $\text{km s}^{-1}$ ]		$1.70^{+0.08}_{-0.09}$

the DE-MCMC algorithm<sup>6</sup>. At this stage, we allow for a free offset parameter for each of the five independent RV datasets. The final likelihood function used in the DE-MCMC analysis is:

$$\ln \mathcal{L} = -\frac{1}{2} \left( \sum_{l=1}^{N_{inst}} \sum_{i=1}^{N_{RV}} \left( \frac{RV_i^{(obs)} + RV_l^{(off)} - RV_i^{(model)}}{\sigma_{RV,i}} \right)^2 + \sum_{j=1}^{N_{astr}} \left( \frac{X_j^{(obs)} - X_j^{(model)}}{\sigma_{X,j}} \right)^2 + \sum_{j=1}^{N_{astr}} \left( \frac{Y_j^{(obs)} - Y_j^{(model)}}{\sigma_{Y,j}} \right)^2 + \sum_{k=1}^3 \left( \frac{\mu_{RA,k}^{(obs)} - \mu_{RA,k}^{(model)}}{\sigma_{\mu_{RA,k}}} \right)^2 + \sum_{k=1}^3 \left( \frac{\mu_{DEC,k}^{(obs)} - \mu_{DEC,k}^{(model)}}{\sigma_{\mu_{DEC,k}}} \right)^2 \right) \quad (4)$$

The DE-MCMC analysis was carried out in the same way as described in the previous section. The final results are reported in Table 8 and Figures A2, A3 and A4, with Figure 6 showing the best-fit solutions for the RV time-series, speckle data (in cartesian coordinates), and absolute astrometry.

The combination of radial velocity data, relative and absolute astrometry is the most complete dataset available to us and the orbital solution presented in Table 8 is the one we consider as final. The orbital elements of the  $\beta$  Cyg A system (both fitted and derived) are all determined within  $1\sigma$  of the values obtained by fitting an orbit only to RVs and speckle imaging data. The orbital configuration is therefore robustly confirmed based on the combined modelling of the three datasets. Also in this case, attempts at fitting shorter- or longer-period orbits as done in Sect. 4.2 confirmed that the solution reported in Table 8 is the one with the higher likelihood.

To further quantify the quality of the global fit, we use the same statistics utilized in Sect. 4.1, i.e. the ratio of the rms of the residuals

<sup>6</sup> For the purpose of this study, in the modelling of the HIPPARCOS-Gaia absolute astrometry of  $\beta$  Cyg Aa we ignore any wavelength-dependent effects on the photocenter due to the presence of  $\beta$  Cyg Ac

of a given dataset to its mean uncertainty: A value close to unity is an indication that the residuals are fully compatible with the reported measurement uncertainties. For the RV datasets, this ratio is always  $< 0.85$ . For the speckle imaging data, we have 0.86 and 1.44 along the X- and Y-axis, respectively. For the absolute astrometry we obtain 0.23 and 2.68 in RA and DEC, respectively. The only discrepant value is the proper motion in DEC at the mean *Gaia* DR2 epoch, not unexpected given the large uncertainties in the astrometric solution for such a bright star.

The values of systemic proper motion and mass ratio are highly correlated, as expected. The  $\mu_{\text{DEC}}^b$  value is compatible at the  $1.6\sigma$  level with the equivalent long-term value for the star in the Tycho-2 catalogue (Høg et al. 2000), while the  $\mu_{\text{RA}}^b$  value obtained in our solution and the Tycho-2 one are discrepant at the  $6.7\sigma$  level. In contrast to the estimate made in the previous subsection, the  $q$  value we obtain in our global solution is distance independent. We find  $q = 1.25^{+0.19}_{-0.16}$ . This value is surprising, as it points to a much larger mass for Albireo Ac than previously thought, or to its possible binarity. As a consequence, the  $K$ -value is also significantly larger than the one obtained in the solution presented in the previous section (Table 7), in part possible now that we have introduced zero-point offsets for each RV dataset, which are found to be within  $1 - 2 \text{ km s}^{-1}$  of the median RV value of each dataset. An additional effect is that the uncertainty on the systemic radial velocity  $\gamma_{\text{sys}}$  (reported in Table 8 as the weighted average of the individual RV zero-points) now realistically includes possible calibration errors.

As shown in Figure A4, the posterior distributions of parallax and total system mass allow us to infer directly from the data that  $\varpi = 6.79^{+1.13}_{-1.11} \text{ mas}$  (and thus  $d = 147.40^{+28.82}_{-21.01} \text{ pc}$ ) and  $M_{\text{tot}} = 14.17^{+9.27}_{-5.19} M_{\odot}$  (with individual component masses  $M_{\text{Aa}} = 6.29^{+4.47}_{-2.47} M_{\odot}$  and  $M_{\text{Ac}} = 7.84^{+4.90}_{-2.74} M_{\odot}$ ).

## 5 DYNAMICAL ANALYSIS OF THE ALBIREO SYSTEM

### 5.1 Direct-measurement approach

Can astrometric or radial-velocity measurements be used to directly confirm that the Albireo triple is gravitationally bound? Let us assume the best-case scenario that all three stars are at the same distance, and that:

- the distance of the system is 120 pc (Section 2.3).
- the masses of the partners are as derived in Section 3 above, i.e. that the total mass of the system is  $11.6 M_{\odot}$ ,
- the separation of the wide pair in the line-of-sight spatial coordinate is equal to the average separation in the two sky plane coordinates, i.e.  $2927 \text{ au}$ , (corresponding to  $34.5 \text{ arcsec}/\sqrt{2}$ ) at 120 pc,
- and that the present 3-dimensional separation following from the above assumptions (namely  $5070 \text{ au}$  or  $0.025 \text{ pc}$ ) is the semi-major axis of the orbit.

Then Kepler's laws give the following measurable parameters (some of them depending on inclination, eccentricity and orbital phase):

- an orbital period of around 106 000 years
- an orbital velocity in the order of  $1.4 \text{ km s}^{-1}$ , of which on average a proportion of  $1/\sqrt{3}$ , i.e.  $0.8 \text{ km s}^{-1}$  would point in the line-of-sight direction (at least in certain orbital phases)
- a relative orbital proper motion in the order of  $2 \text{ mas yr}^{-1}$
- a relative angular acceleration in the order of  $0.12 \mu\text{as yr}^{-2}$
- an orbital acceleration of  $5 \text{ mm s}^{-1} \text{ yr}^{-1}$ .

We note that the difference between the systemic proper motion

**Table 8.** Priors and best-fit results for the DE-MCMC analysis of the combined RV + speckle imaging + absolute astrometry time series. The value of  $\gamma_{\text{sys}}$  is taken as the median of the prior distribution of all the RV offsets.

Jump parameter	Prior	Best-fit value
$P$ [yr]	$\mathcal{U}(100,150)$	$121.45^{+2.80}_{-2.73}$
$T_0$ [yr]	$\mathcal{U}(2000.0,2050.0)$	$2026.44^{+0.98}_{-0.99}$
$e$	$\mathcal{U}(0.0,0.99)$	$0.20^{+0.01}_{-0.02}$
$q$	$\mathcal{U}(0.0,2.0)$	$1.25^{+0.19}_{-0.16}$
$\mu_{\text{RA}}^b$ [mas yr $^{-1}$ ]	$\mathcal{U}(-10.0,10.0)$	$1.22^{+0.22}_{-0.23}$
$\mu_{\text{DEC}}^b$ [mas yr $^{-1}$ ]	$\mathcal{U}(-10.0,10.0)$	$-0.16^{+0.67}_{-0.70}$
$RV_1^{off}$	$\mathcal{U}(-50.0,0.0)$	$-23.92^{+0.10}_{-0.14}$
$RV_2^{off}$	$\mathcal{U}(-50.0,0.0)$	$-25.46^{+0.20}_{-0.13}$
$RV_3^{off}$	$\mathcal{U}(-50.0,0.0)$	$-22.66^{+0.15}_{-0.32}$
$RV_4^{off}$	$\mathcal{U}(-50.0,0.0)$	$-21.59^{+0.16}_{-0.19}$
$RV_5^{off}$	$\mathcal{U}(-50.0,0.0)$	$-23.61^{+0.60}_{-0.53}$
<i>Derived quantities</i>		
$a$ [arcsec]		$0.400^{+0.006}_{-0.005}$
$i$ [deg]		$23.19^{+2.45}_{-2.80}$
$\Omega$ [deg]		$84.16^{+4.62}_{-4.23}$
$\omega$ [deg]		$54.87^{+1.80}_{-1.96}$
$\gamma_{\text{sys}}$ [km s $^{-1}$ ]		$-23.66^{+1.93}_{-1.66}$
$K$ [km s $^{-1}$ ]		$3.26^{+0.15}_{-0.24}$
$\varpi$ [mas]		$6.79^{+1.13}_{-1.11}$
$d$ [pc]		$147.40^{+28.82}_{-21.01}$
$M_{\text{tot}}$ [ $M_{\odot}$ ]		$14.17^{+9.27}_{-5.19}$
$M_{\text{Aa}}$ [ $M_{\odot}$ ]		$6.29^{+4.47}_{-2.47}$
$M_{\text{Ac}}$ [ $M_{\odot}$ ]		$7.84^{+4.90}_{-2.74}$

of  $\beta$  Cyg A and the proper motion of B is indeed of the order of  $2 \text{ mas yr}^{-1}$ . However, as we will see below, the observed difference in the radial velocities of A and B still make it unlikely that these two stars are bound.

### 5.2 Statistical approach

Another approach we can take to study the dynamical state of Albireo is a statistical one. As discussed earlier in this paper, we do not have reliable information concerning the parallax of  $\beta$  Cyg A, and the analysis performed in Section 4.3 resulted in an orbital parallax just significantly smaller than that of  $\beta$  Cyg B. This uncertainty on the parallax translates into a large uncertainty on the line-of-sight separation between  $\beta$  Cyg A and B, which is a key ingredient to determine if the system is gravitationally bound. For these reasons, since it is very difficult to obtain a complete and accurate orbital solution for the Albireo stellar system, we decided to study its dynamical nature via Monte Carlo simulations. Our simulations are loosely based on the combined analysis of RVs and astrometric data in Pinamonti et al. (2018), following the technique from Hauser & Marcy (1999).

We took into account the possible distances and proper motions for  $\beta$  Cyg A derived from the final orbital solution we presented in Sect. 4.3. We adopted the mass value of  $\beta$  Cyg B listed in Table 5, and the positions of the two components from *Gaia* DR2. The proper motion of  $\beta$  Cyg B adopted was that of Brandt (Table 3), while the

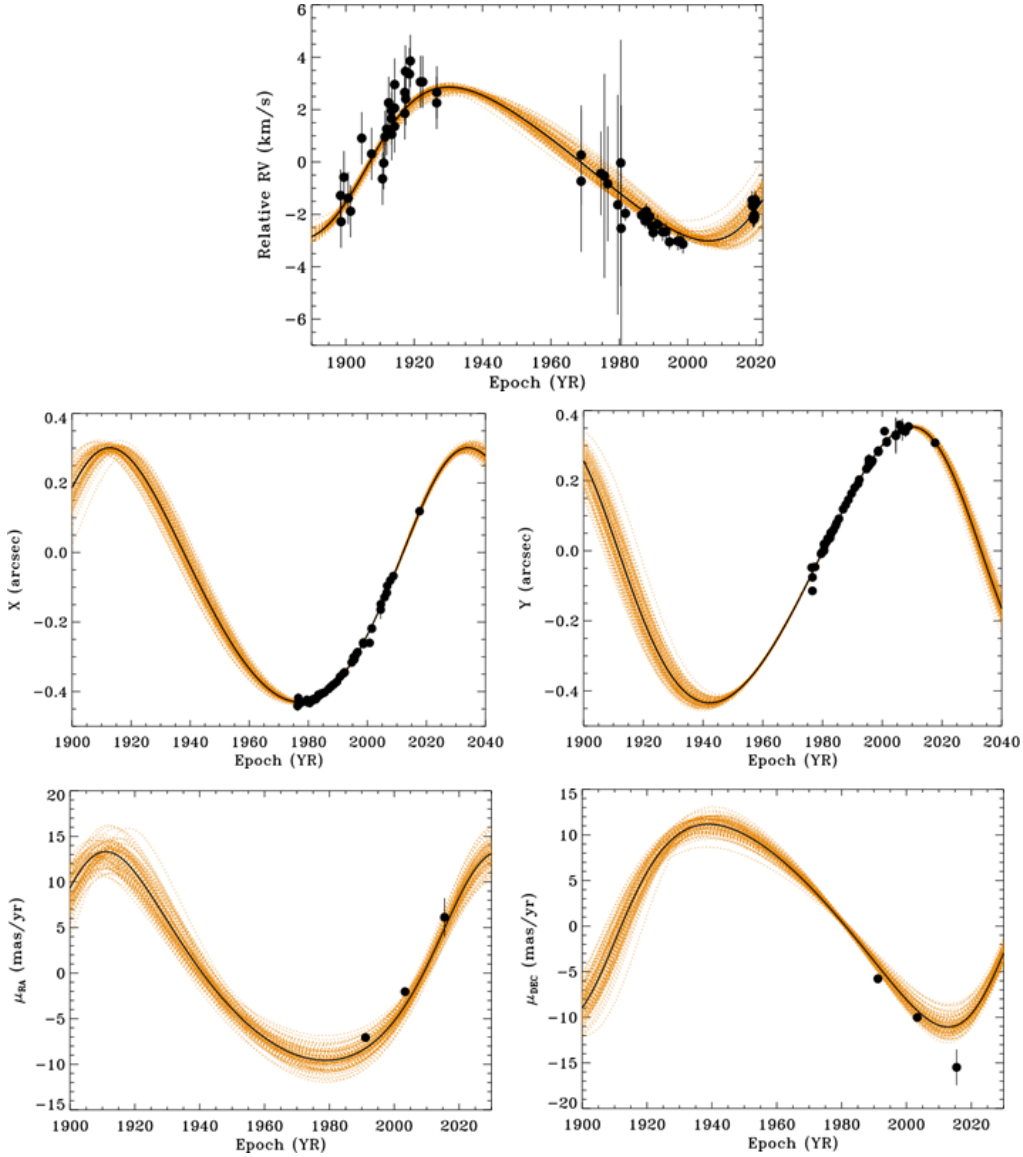


**Figure 6.** The best-fit Keplerian model (solid black line) superposed to the RV time series (top panel), to the speckle imaging data (middle panels), and to the absolute proper motions from *HIPPARCOS* and *Gaia* (lower panel). The dashed orange lines represent a random selection of orbit solutions drawn from our DE-MCMC posteriors.

parallax value adopted of  $\beta$  Cyg B was the weighted mean value derived in Sect. 2.3 ( $8.33 \pm 0.13$  mas). The proper motion and mass for  $\beta$  Cyg A, is obtained from the final orbit solution (Table 8). Since the position in the sky of  $\beta$  Cyg A depends on the orbital motion of the Aa with respect to the barycentre, we added in quadrature the semi-major axis of the orbit to the error on the position given by *Gaia*. We adopted the systemic radial velocity for  $\beta$  Cyg A from Table 8, and the value  $-18.8 \pm 2.20$  km s $^{-1}$  from Kharchenko et al. (2007) for B. We then randomly generated all parameters for  $\beta$  Cyg B, as well as the position of  $\beta$  Cyg A and its radial velocity, with Gaussian distributions centered on the mean value of each parameter and standard deviation equal to their respective uncertainty. The other parameters for  $\beta$  Cyg A (i.e. its parallax, mass, and proper motions) were instead randomly drawn from the posterior distributions obtained from the DE-MCMC analysis in Sect. 4.3, to preserve possible correlations. We generated a sample of 1 000 000 realizations.

Taking into account the possible parallax distribution for  $\beta$  Cyg A

derived in Section 4.3, we can compute the line-of-sight separation  $z$ , and we thus have the complete set of possible relative positions and velocities, as the relative positions in the sky,  $(x, y)$ , of B with respect to A, can be derived from *Gaia* astrometry, and the three components of the relative velocity  $V_x, V_y, V_z$ , from the proper motions and RVs. For the system to be gravitationally bound, the total energy must be negative:

$$E = \frac{1}{2} \frac{M_A M_B}{(M_A + M_B)} v^2 - \frac{G M_A M_B}{r} < 0, \quad (5)$$

where  $r$  and  $v$  are the relative positions and velocities of B with respect to A.

We then study the distribution of parallaxes and masses of  $\beta$  Cyg A for the bound systems, which are shown in Fig. 7, compared to the general distribution of parallaxes and masses resulting from the analysis in Sect. 4.3. It is worth noticing that the fraction of bound solutions is very small, with less than 0.01% of the systems gravitationally bound, and that they are all concentrated in a very

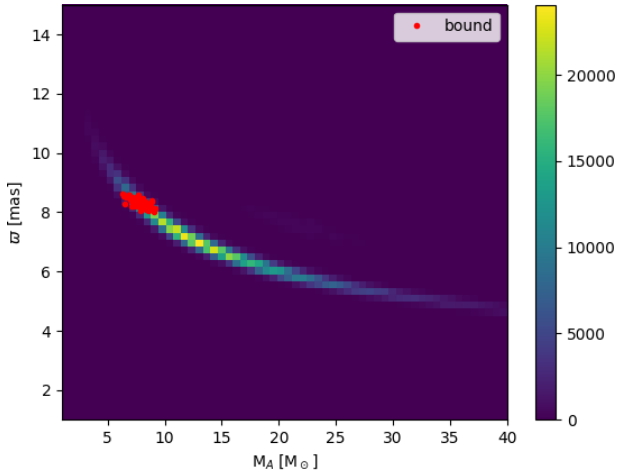


**Figure 7.** Probability density of possible  $\beta$  Cyg A parallaxes  $\pi_A$  and masses  $M_A$  for the complete sample drawn from the posteriors of the DE-MCMC model from Sect. 4.3. The red dots mark the subset of solutions resulting in  $\beta$  Cyg A and B being bound.

small island of the parameter space. The set of bound solutions always correspond to cases in which the parallax of  $\beta$  Cyg A is very close to the value of  $\beta$  Cyg B ( $\varpi_{A,\text{bound}} = 8.30^{+0.18}_{-0.15}$  mas) and with a total mass much smaller than the best fit value for  $M_{\text{tot}}$  listed in Table 8 ( $M_{A,\text{bound}} = 7.85^{+0.80}_{-0.74} M_{\odot}$ ), even if not strongly significant due to the large uncertainties in Table 8. In particular, it is interesting to notice that this value is very close to the spectroscopic estimate of the total stellar mass of  $\beta$  Cyg A determined in section 3, computed by adding the values in Table 5. However, the mass ratios of these bound systems is nevertheless found to be  $q = 1.32^{+0.11}_{-0.14}$ , inconsistent with of the mass ratio obtained from the same values in Table 5, but instead very close to the value obtained in Sect. 4.3.

As an additional test, we studied this best-case region of the parallax-mass parameter space that allows bound orbits, to better understand the influence of the other parameters on the dynamical state of the system, in particular of the relative velocity of the two components. For this test the mass value of  $\beta$  Cyg A listed in Table 5 is used, since it was very close to the value obtained above for the bound solutions, and we randomly generated its values with a Gaussian distribution, instead of drawing them from the posterior as previously done.

We then derived as before the relative positions in the sky,  $(x, y)$ , and the three components of the relative velocity  $V_x, V_y, V_z$ . Without constraining the separation along the line-of-sight  $z$ , we can study the minimum energy of the system  $E_{\text{min}}$ , computed by substituting  $r = \sqrt{x^2 + y^2 + z^2}$  in Eq. 5 with  $r_{xy} = \sqrt{x^2 + y^2}$ . If  $E_{\text{min}} > 0$  there will be no possible value of  $z$  for which the system is bound. Figure 8 shows the distribution of the relative line-of-sight velocity  $V_z$  for the total sample and for the subsample of potentially bound systems where  $E_{\text{min}} < 0$ . In only 12.4% of the realizations the system could be bound, and they all correspond to values of  $V_z$  much closer to zero than the mean value:  $V_{z,\text{bound}} = 0.72^{+0.76}_{-1.12} \text{ km s}^{-1}$ . This suggests that, even in the best-case scenario in which the two components are nearly at the same distance, the observed difference in the relative line-of-sight velocity allows only a 1 in 8 possibility that A and B are bound.

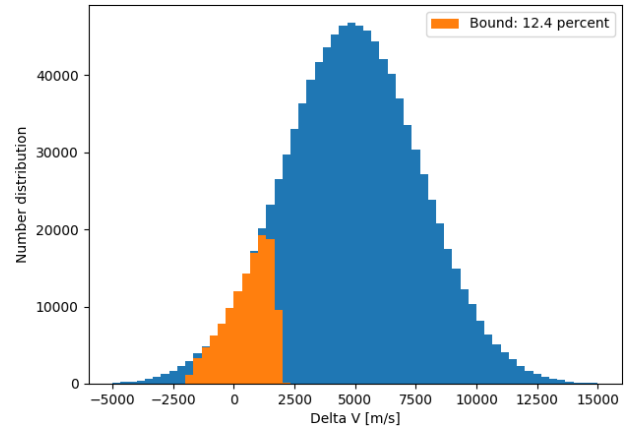


**Figure 8.** Distribution of possible relative line-of-sight velocities  $V_z$  between  $\beta$  Cyg A and B (blue) and the subset of these relative velocities that potentially allow bound orbits.

### 5.3 Motion of the Albireo system

With estimated mass for  $\beta$  Cyg A and B, as well as their proper motion, we can infer the proper motion of the Albireo system, that is, of its barycentre. If the two stars are bound their orbital velocities, with respect to the barycentre, are in opposite directions, and in consequence the components of these velocities tangent to our line-of-sight. In addition, the ratio of the magnitudes of these velocities as the inverse ratio of their masses. These assumptions are also valid if A and B have recently become unbound, that is, their velocities with respect to their barycentre will be in opposite directions and their ratio as the inverse of their masses. If A and B are bound we can (and should) assume that they are at the same distance, so that the ratio of the projected orbital velocities also holds for their orbital proper motions, that is

$$\frac{\|\vec{\mu}_a\|}{\|\vec{\mu}_b\|} = \frac{M_B}{M_A} \equiv q_{AB}, \quad (6)$$

where  $\vec{\mu}_a$  and  $\vec{\mu}_b$  are the orbital proper motions of A and B with respect to their barycentre. These ratios will hold also for the unbound case, if the separation of A and B is negligible with respect to their distance. We can thus decompose the total proper motion into two components: the proper motion of the barycentre,  $\vec{\mu}_s$ , and the orbital proper motion from the velocity with respect to the barycentre. That is, the systemic proper motion of the  $\beta$  Cyg A system is:

$$\vec{\mu}_A = \vec{\mu}_s + \vec{\mu}_a, \quad (7)$$

where  $\vec{\mu}_a$  the component of this proper motion due to its velocity with respect to the barycentre of Albireo, and similarly for  $\vec{\mu}_b$ . Using the above ratio and solving for  $\vec{\mu}_s$  we have

$$\vec{\mu}_s = \vec{\mu}_B + \frac{(\vec{\mu}_A - \vec{\mu}_B)}{(1 + q_{AB})}, \quad (8)$$

keeping in mind that the orbital proper motions are in opposite directions, that is,  $\vec{\mu}_a = -q_{AB}\vec{\mu}_b$ . Now for  $\beta$  Cyg A we consider two possible masses. If bound and/or at the same distance as  $\beta$  Cyg B,  $M_A = 7.9 M_{\odot}$ . Otherwise we can assume  $M_A = 14.2 M_{\odot}$ , as estimated in Section 4.3. In the first case we find the proper motion of the Albireo system to be  $\vec{\mu}_s = (0.50, -0.57) \text{ mas yr}^{-1}$ , while in the second case it is  $\vec{\mu}_s = (0.76, -0.42) \text{ mas yr}^{-1}$ .



## 6 KINEMATIC ANALYSIS OF THE ALBIREO SYSTEM: RELATION BETWEEN $\beta$ Cyg A AND $\beta$ Cyg B

In the previous section we showed that, given our current observations,  $\beta$  Cyg A and B are very unlikely to be a bound system. Or, if one prefers, that our current observations are unable to resolve the question of whether they are bound or not. In any case, the more relevant scientific question is not whether  $\beta$  Cyg A and B are currently gravitationally bound or not, but whether they have a common history, age and origin. Under the assumption that they are at the same distance, section 3.4 shows that  $\beta$  Cyg A and B are coeval, but in fact we do not know that A and B are at the same distance. In the following we will show that the question of having a common origin can be answered in the affirmative, by a probabilistic approach, and to a very high probability.

The century-old discussion whether Albireo A and B are physically connected or merely a coincidental optical double is based on their angular proximity on the sky. But, somewhat surprisingly, this argument apparently has never been elaborated quantitatively. By doing so, the question could have been largely settled already 22 years ago, in a probabilistic way.

### 6.1 Two dimensions

The HIPPARCOS Catalogue by definition includes a complete celestial census down to apparent magnitude  $V=7.9$ . Thus by construction it contains a complete census of all B stars out to distances well beyond Albireo's: The absolute magnitude of an A0 star is  $M_V=+0.6$ , thus it reaches apparent magnitude  $V=7.9^7$  at 290 pc.

The New Reduction of the HIPPARCOS Catalogue (van Leeuwen 2007) contains 37696 stars with  $\varpi > 7.0$  mas. Using the compilation by Anderson & Francis (2012), we find that among these there are 591 B stars of all types, distributed almost evenly over the whole sky. For any given member of this set, the probability to find another unrelated member within 34.5 arcsec is only  $1.3 \times 10^{-6}$  (590 times the solid angle covered by a circle of radius 34.5 arcsec divided by the  $4\pi$  radians of the whole sky). Thus already from this simple two-dimensional argument alone, the credibility of a physical connection between Albireo A and B is very high by all scientific standards.

### 6.2 Three, five and six dimensions

This low probability of an optical pair can even be further reduced by introducing additional observed quantities to the argument.

Firstly, the distances of the two stars are roughly equal. Taking the least favourable combination of measured parallaxes for A and B, namely the *Gaia* DR2 ones, we can omit the inner part of the narrow spatial cone set by the positional agreement on the sky. This reduces the probability derived in Section 6.1 above by a mild factor of 0.6.

Secondly, and more importantly, the proper motions are roughly equal, too. The proper motion of  $\beta$  Cyg B is indisputably close to the *Gaia* DR2 value of  $(-1, -0.5)$  mas yr $^{-1}$ , to within 1 mas yr $^{-1}$ . Above, we determined the systemic motion of Albireo A to be about  $(1.22 \pm 0.2, -0.16 \pm 0.7)$  mas yr $^{-1}$  (Table 8). At 120 pc distance, the total proper-motion difference of about 2.3 mas yr $^{-1}$  translates into a difference of tangential velocity by only 1.3 km s $^{-1}$ . This small difference must be compared with the velocity dispersion of young stars

in the solar neighbourhood, which is slightly below 10 km s $^{-1}$  in all three spatial dimensions (Binney et al. 2000).

Assuming the dispersion of  $\sigma_v = 10$  km s $^{-1}$ , a conservative estimate of the probability of finding a coincidental partner to a given star within an interval  $\pm \Delta v_t$  can be computed from the density function of a Gaussian distribution near its centre:  $dP/dv = (\sqrt{2\pi}\sigma_v)^{-1}$ . Applying this to both coordinates of the tangential velocity (using the uncertainty rather than the actual small value of the difference in declination), and multiplying with the 2-d probability found above, the total probability for an unrelated optical pair Albireo AB is reduced to  $1.3 \times 10^{-8}$ . Adding the less precise difference in radial velocity to the argument, the probability is lowered further, to  $5 \times 10^{-9}$ .

This means — to a very high probability — that the wide pair of the Albireo system, even if unbound, very likely has a common origin and is indeed coeval.

### 6.3 A possible Albireo moving group

A third — less quantitative, but scientifically even more interesting — way to argue for a physical connection between Albireo A and B would be the detection of an entire moving group or star cluster at the same distance and space velocity. We therefore conducted a careful search for possible additional members of the Albireo system. This search was in part motivated by the recent discovery of a formidable star cluster around another pair of B stars, namely  $\beta$  Lyrae (Bastian 2019), the long-known existence of a similar cluster around the pair  $\delta$  Lyrae, and of several moving groups around other B stars.

Drawing a tight 3-dimensional box around the HIPPARCOS parallax of Albireo B and the proper motion of the Albireo system,  $\vec{\mu}_s = (0.50, -0.57)$  mas yr $^{-1}$  (see Section 5.3), we found four more stars (in addition to Albireo B) in a circle of 5 degrees around the position of Albireo on the sky. Three of them lie within 0.8 degrees from that position. The additional members of the group are listed in Table 9. Details on their selection are given in the Appendix.

As explained in the Appendix, the expected number of stars in the box is only 0.017 stars within the 0.8 degree radius, and 0.37 stars within the 3.7 degree radius. So, we have a strong over-density, especially in the smaller circle on the sky. The Poissonian probabilities of finding three stars in the smaller and four stars in the larger circle are  $9 \times 10^{-7}$  and  $5 \times 10^{-4}$ , respectively. Thus, with quite high probability we have identified a sparse, but spatially well concentrated moving group surrounding the long-known triple (now probably quadruple) Albireo system. This lends additional credibility to the physical connection of Albireo A and B.

The reality of the moving group could be confirmed beyond any reasonable doubt by measuring the sixth phase space component, namely the radial velocity, of the four suspected members. A moderate precision of 1-2 km s $^{-1}$  would be sufficient. But due to the faintness of the stars, this task is outside the scope of the present study.

In passing we note that the Jacobi limit (“tidal radius”) of a stellar system of  $11.6 M_\odot$ , i.e. having the sum of the masses of Albireo Aa+Ac+B derived from the spectroscopy in section 3 (Table 5), is about 3.0 pc. At 120 pc distance this translates into 1.5 degrees. This means that three out of our four member candidates are well within this limit, and the fourth one marginally outside. Members of a bound system are expected to be found mainly within two Jacobi radii from the center of mass, i.e. within 3 degrees in this case.

<sup>7</sup> Note that interstellar extinction is negligible within 120 pc on the whole sky.

**Table 9.** The candidate members of the suspected Albireo moving group. The columns give the *Gaia* DR2 star number, right ascension and declination, parallax, magnitude, colour and angular separation from Albireo.

SourceId <i>Gaia</i> DR2	alpha degrees	delta degrees	parallax mas	G mag	BP-RP mag	rho degrees
2026157766897183360	292.2059	28.1536	7.9	14.7	2.4	0.4
2026178417101258624	292.7363	28.3575	8.3	15.9	2.8	0.4
2026300016218003072	292.7387	28.7854	8.3	13.6	1.9	0.8
2032809846604646400	293.7991	31.2592	8.2	17.1	3.1	3.7

## 7 EVIDENCE OF HIDDEN MASS IN $\beta$ Cyg A

As shown in section 3, the properties of the known stellar components of the Albireo system are consistent with it being coeval, with an age of 99 Myr, under the hypothesis that all stars in the  $\beta$  Cyg A system are at the same distance (120 pc). This result is also consistent with the orbital solution derived from the radial velocity data and (relative) speckle astrometry (section 4.2) which, if assuming a distance of 120 pc, results in a mass ratio for  $\beta$  Cyg Aa/Ac of  $q = 0.53^{+0.13}_{-0.09}$ , consistent with the value of  $q = 0.52$  derived from the spectroscopic/photometric analysis under the same hypothesis. Only one detail seems out of place, namely the derived luminosity and temperature of Ac is not as expected for a star of 99 Myr. This can be considered a minor inconsistency, given the large uncertainties in the derived stellar parameters of Ac, unavoidable given its proximity to Aa.

This tidy picture is completely disrupted when we bring in the absolute astrometry, which allows us to derive an orbit solution completely consistent with the radial velocity and speckle data, but which gives us a mass ratio of  $q = 1.25^{+0.19}_{-0.16}$ , a total mass of  $M_{\text{tot}} = 14.17^{+9.27}_{-5.19} M_{\odot}$  for the  $\beta$  Cyg A system, and an orbital parallax that implies that the separation between Albireo A and B is 20–30 pc. Only in the case that A and B are indeed at the same distance would the total mass for A agree with that estimated from spectroscopy, though even here the astrometry indicates that  $q > 1$ , inconsistent with the individual masses estimated in Section 3.4 that suggest  $q = 0.53$ .

Might there be problems with the absolute astrometry from either HIPPARCOS or *Gaia*, or has our interpretation of the absolute astrometry gone astray?

For HIPPARCOS, the  $\beta$  Cyg A system is unresolved and, notwithstanding its brightness, should not present particular measurement problems. For *Gaia*,  $\beta$  Cyg A is more problematic, given its brightness as well as the fact that, with a separation of  $\approx 0.4$  arcsec, the system is marginally resolvable, if the fainter member is not completely lost in the glare of the primary. These effects might introduce important bias in both the *Gaia* measured proper motions and parallax, but should not introduce bias in the measured position. However, we stress that our result does not depend on the *Gaia* proper motion. Indeed, the mass ratio  $q$  and systemic proper motion can be analytically solved for using only the HIPPARCOS and Brandt proper motions, the latter depending only on the *Gaia* position, together with the relative proper motion and displacement of the secondary (Ac) with respect to the primary (Aa) at the HIPPARCOS epoch, based on the fit to the speckle data. One can show that

$$Q \equiv \frac{q}{1+q} = \frac{\|\vec{\mu}_B - \vec{\mu}_H\|}{\|\vec{\mu}_h - \frac{\Delta\vec{x}_{\text{rel}}}{\Delta t_{HG}}\|}, \quad (9)$$

where  $\Delta\vec{x}_{\text{rel}}$  is the relative displacement vector of Ac between the *Gaia* and HIPPARCOS epochs, and  $\Delta t_{HG} = 24.25$  yrs is the difference

between the HIPPARCOS and *Gaia* DR2 epochs. From the relative orbit solution we have  $\vec{\mu}_h = (15.24, 10.88) \text{ mas yr}^{-1}$  and  $\Delta\vec{x}_{\text{rel}} = (0.141, 0.431) \text{ arcsec}$ , giving us  $q = 1.26$  and a systemic proper motion of  $(1.208, -0.105) \text{ mas yr}^{-1}$ , in complete agreement with the solution derived in section 4.3. That the *Gaia* proper motion has little weight in the final orbit solution is a consequence of the larger (inflated) uncertainties assigned to these measurements.

This leaves us with possible problems in our analysis, and in particular our assumptions. We have assumed that HIPPARCOS and *Gaia* are both measuring the position of the primary, Aa, that is, the measured photocenter corresponds to the position of Aa. However, a more careful analysis, taking into account the flux ratio of the two components in the HIPPARCOS and *Gaia* passbands, would only make  $q$  even larger, exasperating the problem of needing additional mass in the Ac component.

We've also assumed that the speckle reference frame is the same as that of HIPPARCOS and *Gaia*. However, we expect that at most there may be a rotation between the two frames no larger than  $\delta\theta = 0.1^\circ$ , leading to corrections of the order of  $\rho \sin \delta\theta = 0.7 \text{ mas}$  (where  $\rho = 40 \text{ mas}$  is the angular separation of Aa/Ac), which is much too small to possibly account for large systematic errors in the astrometry.

Trusting our results, we conclude that the absolute astrometry from HIPPARCOS and *Gaia* indicate that there is likely hidden mass in the  $\beta$  Cyg A system.

One obvious way to increase the mass of Ac without offending the observations is to hypothesize that it is itself a binary. The maximum mass for Ac would be an equal-mass binary with two stars of half the luminosity as observed for Ac, which would also explain its over-luminosity. At a distance of 120 pc a star with half the luminosity of Ac would have a mass of  $2.25 M_{\odot}$ , bringing the total mass of  $\beta$  Cyg A to  $9.7 M_{\odot}$  and raising  $q$  to 0.87. This would bring the total mass to within one sigma of the total mass determined using the absolute astrometry, but still outside the expected range for  $q$ ,  $(1.25^{+0.19}_{-0.16})$ .

If however  $\beta$  Cyg A is more distant than B, as suggested by our final orbit solution, then both Aa and Ac will be more luminous. The primary Aa would, consequently, be more massive but still coincide, within the uncertainties, with the age of B. At 133 pc distance, as indicated by HIPPARCOS for example, we obtain a mass of Aa of  $5.7 M_{\odot}$  with an age of 90 Myrs. However, Ac would now fit on a main sequence evolution track of  $3.0 M_{\odot}$ , but even further from the then relevant 90 Myr isochrone.

Another, more exotic, solution to our missing mass problem is that the light from Ac comes from a star with a black-hole companion. This hypothesis might also explain the anomalous temperature/luminosity of Ac, which indicates that it is more evolved than expected from an 99 Myr isochrone. A search for corroborating evidence in NASA's HEASARC database does not reveal  $\beta$  Cyg A as being a high-energy source, however such emission is only expected if mass transfer has created an accretion disk about the black hole, and indeed is absent in known systems with candidate stellar mass

black holes (Rivinius et al. 2020; Liu et al. 2019). Assuming the total mass of  $7.8 M_{\odot}$  for Ac derived in Sect. 4.2 is the sum of the  $2.7 M_{\odot}$  luminous component and a  $5.1 M_{\odot}$  dark companion, we used a standard injection and recovery method of synthetic signals (see e.g. Mortier et al. 2012) in the residuals of the speckle relative astrometry to place an upper limit to the maximum separation between the black hole and the stellar companion. We find that, for assumed system distances of 140 pc and 120 pc and averaging over all orbital elements, we would have detected (at the 95% confidence level) clear periodicities in the residuals for orbital periods  $> 1.5$  yr and  $> 0.9$  yr, respectively, corresponding to angular orbit sizes of  $\gtrsim 15$  mas (approximately twice the size of the rms of speckle astrometry residuals). Based on a Generalized Lomb Scargle periodogram analysis (Zechmeister & Kürster 2009), we see no evidence of periodic motion in the residuals of the speckle data, therefore the companion must have a significantly shorter orbital period.

Evidence of an unseen high-mass companion to Ac would be confirmed if Ac’s radial velocity significantly differed from that of Aa. A search of the literature for radial velocity measurements of Ac, whose Balmer series is clearly visible in the  $\beta$  Cyg A spectrum, resulted in only one find: eight measures by E. Hendry, published with her measurements of the primary (Hendry 1981). These measurements are, not surprisingly, rather uncertain, but show a significant variance. However their mean is also significantly biased with respect to the systemic radial velocity of  $\beta$  Cyg A, bringing into question their reliability. Given that no others in the field have dared to measure (or publish) is a good indication of the challenge of measuring Ac’s radial velocity, but if indeed Ac has a black hole as a companion, high precision might not be needed if the orbital inclination is not small.

We note that there are also LWP and SWP high-resolution spectra from the 1980’s in the IUE archive, which should be dominated by the flux from the hotter Ac component. We did not consider using this potential radial velocity information as the read-out of the reticon cameras of IUE was rather noisy: Even in well exposed spectra, signal-to-noise rarely exceeds 20. More importantly the spectral resolving power of the high-resolution mode is also very modest by today’s standards, varying between 12,000 and 15,000. This results in a measurement error of up to  $0.07 \text{ \AA}$  (for details, see Boggess et al. (1978)), or  $7$  to  $10 \text{ km s}^{-1}$ , much larger than the amplitude of the orbital velocity expected from the Aa/Ac pair alone. However, given the possibility that orbital motion with a close unseen companion might be detected, it may be worth reconsidering these measurements.

In any case, our determination of the total mass of the  $\beta$  Cyg A system based on the astrometry and radial velocity data indicates that there is likely a fourth, hidden component, making Albireo a hierarchical quadruple system.

## 8 CONCLUSIONS

We have here presented the first well-constrained orbit solution for the close binary comprising the primary of the wide pair of the Albireo system,  $\beta$  Cyg A, finding a period of  $121.45^{+2.8}_{-2.7}$  yr and low eccentricity. This is mainly accomplished by combining the speckle data, providing relative astrometry over about one fourth of its orbit, with radial velocity measurements spanning a baseline of more than 120 years.

With the addition of absolute astrometry from HIPPARCOS and Gaia, we are also able to estimate the systemic proper motion of  $\beta$  Cyg A and the mass ratio of the Aa/Ac pair, as well as the total mass of the system. Our final orbit solution also gives an orbital parallax estimate. Our determination of the systemic motion

of  $\beta$  Cyg A,  $(1.22 \pm 0.2, -0.16 \pm 0.7) \text{ mas yr}^{-1}$ , is in good agreement with the existing long-term measurements of the proper motion in e.g. FK4 and FK5<sup>8</sup>, and our estimated orbital parallax for  $\beta$  Cyg A,  $6.79 \pm 1.1 \text{ mas}$ , is in good agreement with the New HIPPARCOS measure of  $7.51 \pm 0.33 \text{ mas}$ . Our parallax for  $\beta$  Cyg A suggests that the line-of-sight distance between the A and B components of Albireo may be 20 pc, or even larger, with the implication that A and B are very likely unbound. Nevertheless, such a separation is not in conflict with the hypothesis that these stars were born from the same birth cluster: Consider a common formation of the triple, but in a kinematic configuration that was unbound from the very beginning. The velocity spread in unbound star-forming complexes is in the range of  $0.5$  to  $1 \text{ km s}^{-1}$  typically. An initial velocity difference of only  $0.2 \text{ km s}^{-1}$  would have separated the two partners by a full 20 pc over the past 100 million years.

On the other hand, our final orbit solution for the  $\beta$  Cyg Aa/Ac system does not exclude the possibility that A and B are indeed bound, though our current measurements make this a very unlikely possibility. Clarifying the dynamical state of this system will require not only more precise astrometry, but better radial velocity determinations for both A and B.

Regardless of whether the A and B components are bound, we find there is a very low probability of Albireo A and B being a chance alignment of unrelated stars. This purely statistical argument based on the kinematics and positions of A and B is strengthened by the discovery of a few more stars that seem to be associated with the wide pair. Altogether, this indicates that the Albireo system is the residual massive core of a sparse dissolved — or still dissolving — star cluster.

The most interesting finding of the present study is the surprising fact that Albireo Ac is significantly more massive than Albireo Aa. This is in stark contrast to the photometric and spectroscopic analysis — if Ac is considered to be a single star. It should be pointed out that our finding is very robust: It is independent of the assumed parallax. It is also independent of the orbit solution; it can be directly deduced from a comparison of the relative motion of Ac with respect to Aa, as traced by the speckle data (Figs. 1 and 2), with the Gaia and HIPPARCOS absolute proper motions of Aa. It is even independent of the Gaia DR2 proper motion, as it clearly stands out from the HIPPARCOS and Brandt proper motions alone (as described in Section 7).

Based on the data at our disposal, the additional mass of Ac is best interpreted in terms of the presence of a companion, suggesting that  $\beta$  Cyg A may in fact be a triple system. If we trust the orbital parallax estimate (corroborated by its agreement with the Hipparcos-based direct measurement), it is difficult to reconcile the photometric and spectroscopic data available with the presence of a second luminous, massive component. This raises the intriguing possibility that Ac might be orbiting a dormant, stellar-mass black hole. The nature of the additional mass in Albireo Ac cannot be conclusively determined for the time being, but promising paths towards clarification do exist: these include targeting Albireo Ac with high-contrast imaging observations, adaptive-optics spectroscopy, radial velocity measurements, and very high-resolution interferometric astrometry.

The foundation of these central findings consists of three parts: the robust new orbital solution including the measured radial velocities and relative astrometry from speckle data, the careful spectroscopic confirmation of the physical parameters of the observable stars, and

<sup>8</sup> These two values, despite being derived from observations over more than a century, will still contain some portion of the averaged relative motion due to the 120-year orbit.

the inclusion of the absolute astrometry from HIPPARCOS and *Gaia*. The surprising mass ratio of Aa/Ac had already been found by Bastian & Anton (2018), who could not resolve the mystery at the time because they neither had the correct orbit, nor the new astrophysical information.

We can make a number of predictions for *Gaia* DR3 which — if they hold — will support our findings. They are: the parallax of A and B should become more consistent than seen in DR2, the parallax of A becoming less problematic, and the presently discrepant proper motion in declination should be corrected for Aa, becoming more consistent with that predicted by our final orbit solution, and the kinematic and spatial proximity of additional faint partners should be sharpened and confirmed. The increased precision and reliability of the *Gaia* EDR3 proper motions with respect to DR2 will allow them to significantly improve and confirm the anomalous mass ratio of the stars in the  $\beta$  Cyg A system, as well as the total mass and orbital parallax of the system.

## ACKNOWLEDGEMENTS

A special thanks to Benoit Famaey for sharing CORAVEL data, to Marco Scardia for sharing the latest PISCO measurement and useful discussions, and to Elaine Hendry for clarifications on her observations. This work has made use of data from the European Space Agency (ESA) mission *Gaia* (<https://www.cosmos.esa.int/gaia>), processed by the *Gaia* Data Processing and Analysis Consortium (DPAC, <https://www.cosmos.esa.int/web/gaia/dpac/consortium>). Funding for the DPAC has been provided by national institutions, in particular the institutions participating in the *Gaia* Multilateral Agreement. KS acknowledges support from the CONACyT-DFG bilateral project No. 278156. MP acknowledges financial support from the ASI-INAF agreement n. 2018-16-HH.0.

## DATA AVAILABILITY

All data used in this paper is presented in tabular format in section 2. The spectra for which the HEROS radial velocities are based are available from the authors on request.

## REFERENCES

- Anderson E., Francis C., 2012, *Astronomy Letters*, 38, 331
- Bastian U., 2019, *A&A*, 630, L8
- Bastian U., Anton R., 2018, *A&A*, 620, L2
- Binnendijk L., 1960, Properties of double stars; a survey of parallaxes and orbits.
- Binney J., Dehnen W., Bertelli G., 2000, *MNRAS*, 318, 658
- Blanco-Cuaresma S., 2019, *MNRAS*, 486, 2075
- Blanco-Cuaresma S., Soubiran C., Heiter U., Jofré P., 2014, *A&A*, 569, A111
- Boggess A., et al., 1978, *Nature*, 275, 372
- Brandt T. D., 2018, *ApJS*, 239, 31
- Brandt T. D., 2019, *ApJS*
- Brandt T. D., Dupuy T. J., Bowler B. P., 2019, *AJ*, 158, 140
- Calissendorff P., Janson M., 2018, *A&A*, 615, A149
- Campbell W. W., 1928, Publications of Lick Observatory, 16, 1
- Casertano S., et al., 2008, *A&A*, 482, 699
- Clerke A. M., 1899, *The Observatory*, 22, 387
- Damasso M., et al., 2020, arXiv e-prints, p. arXiv:2007.06410
- De Rosa R. J., Dawson R., Nielsen E. L., 2020, arXiv e-prints, p. arXiv:2007.08549
- Drimmel R., Bucciarelli B., Inno L., 2019, *Research Notes of the American Astronomical Society*, 3, 79
- Dupuy T. J., Brandt T. D., Kratter K. M., Bowler B. P., 2019, *ApJ*, 871, L4
- Eastman J., Gaudi B. S., Agol E., 2013, *PASP*, 125, 83
- Feng F., Anglada-Escudé G., Tuomi M., Jones H. R. A., Chanamé J., Butler P. R., Janson M., 2019, *MNRAS*, 490, 5002
- Flower P. J., 1996, *ApJ*, 469, 355
- Ford E. B., 2006, *ApJ*, 642, 505
- Foreman-Mackey D., Hogg D. W., Lang D., Goodman J., 2013, *PASP*, 125, 306
- Gilmore G., et al., 2012, *The Messenger*, 147, 25
- Grandjean A., et al., 2019, *A&A*, 629, C1
- Gray R. O., Corbally C. J., 1994, *AJ*, 107, 742
- Grevesse N., Asplund M., Sauval A. J., 2007, *Space Sci. Rev.*, 130, 105
- Gustafsson B., Edvardsson B., Eriksson K., Jørgensen U. G., Nordlund Å., Plez B., 2008, *A&A*, 486, 951
- Hartkopf W. I., 1999, IAU Commission on Double Stars, 139, 2
- Hartkopf W. I., et al., 2000, *AJ*, 119, 3084
- Hartkopf W. I., McAlister H. A., Mason B. D., 2001, *AJ*, 122, 3480
- Hauser H. M., Marcy G. W., 1999, *PASP*, 111, 321
- Hendry E. M., 1981, *Publications of the Astronomical Society of the Pacific*, 93, 323
- Høg E., et al., 2000, *A&A*, 355, L27
- Husser T. O., Wende-von Berg S., Dreizler S., Homeier D., Reiners A., Barman T., Hauschildt P. H., 2013, *A&A*, 553, A6
- Jack D., Schröder K.-P., Bastian U., 2018, *Research Notes of the American Astronomical Society*, 2, 225
- Kervella P., Arenou F., Mignard F., Thévenin F., 2019, *A&A*, 623, A72
- Kervella P., Arenou F., Schneider J., 2020, *A&A*, 635, L14
- Kharchenko N. V., Scholz R. D., Piskunov A. E., Röser S., Schilbach E., 2007, *Astronomische Nachrichten*, 328, 889
- Levenhagen R. S., Leister N. V., 2004, *AJ*, 127, 1176
- Lindgren L., 2020a, *A&A*, 633, A1
- Lindgren L., 2020b, *A&A*, 637, C5
- Liu J., et al., 2019, *Nature*, 575, 618
- Makarov V. V., Kaplan G. H., 2005, *AJ*, 129, 2420
- Markowitz A. H., 1969, PhD thesis, THE OHIO STATE UNIVERSITY.
- Maury A. C., Pickering E. C., 1897, *Annals of Harvard College Observatory*, 28, 1
- Mendez R. A., Claveria R. M., Orchard M. E., Silva J. F., 2017, *AJ*, 154, 187
- Mittag M., Hempelmann A., Fuhrmeister B., Czesla S., Schmitt J. H. M. M., 2018, *Astronomische Nachrichten*, 339, 53
- Mortier A., Santos N. C., Sozzetti A., Mayor M., Latham D., Bonfils X., Udry S., 2012, *A&A*, 543, A45
- Parsons S. B., Ake T. B., 1998, *The Astrophysical Journal Supplement Series*, 119, 83
- Perryman M. A. C., et al., 1997, *A&A*, 500, 501
- Pinamonti M., et al., 2018, *A&A*, 617, A104
- Pols O. R., Tout C. A., Schröder K.-P., Eggleton P. P., Manners J., 1997, *MNRAS*, 289, 869
- Pourbaix D., Jorissen A., 2000, *A&AS*, 145, 161
- Randich S., Gilmore G., Gaia-ESO Consortium 2013, *The Messenger*, 154, 47
- Rivinius T., Baade D., Hadrava P., Heida M., Klement R., 2020, *A&A*, 637, L3
- Roberts L. C., Mason B. D., 2018, *MNRAS*, 473, 4497
- Scardia M., et al., 2007, *MNRAS*, 374, 965
- Scardia M., et al., 2019, IAU Commission G1, 198, 3
- Schmitt J. H. M. M., et al., 2014, *Astronomische Nachrichten*, 335, 787
- Schröder K.-P., Pols O. R., Eggleton P. P., 1997, *MNRAS*, 285, 696
- Schröder K.-P., Mittag M., Flor Torres L., Jack D., Snelles I., 2020a, *MNRAS*, in print
- Schröder K. P., Mittag M., Jack D., Rodríguez Jiménez A., Schmitt J. H. M. M., 2020b, *MNRAS*, 492, 1110
- Schwarz G., 1978, *Annals of Statistics*, 6, 461
- Snellen I. A. G., Brown A. G. A., 2018, *Nature Astronomy*, 2, 883
- Ter Braak C. J. F., 2006, *Statistics and Computing*, 16, 239
- Tokovinin A., Hartung M., Hayward T. L., Makarov V. V., 2012, *AJ*, 144, 7
- Wielen R., Dettbarn C., Jahreiß H., Lenhardt H., Schwan H., Jähring R., 2000, in IAU Symposium. p. 144 (arXiv:astro-ph/0004142)



- Wilson R. E., 1953, Carnegie Institute Washington D.C. Publication, p. 0  
 Wright J. T., Howard A. W., 2009, *ApJS*, **182**, 205  
 Xuan J. W., Wyatt M. C., 2020, *MNRAS*, **497**, 2096  
 Zechmeister M., Kürster M., 2009, *A&A*, **496**, 577  
 ten Brummelaar T., Mason B. D., McAlister H. A., Roberts Lewis C. J., Turner N. H., Hartkopf W. I., Bagnuolo William G. J., 2000, *AJ*, **119**, 2403  
 van Leeuwen F., 2007, Hipparcos, the New Reduction of the Raw Data. Vol. 350, doi:10.1007/978-1-4020-6342-8,

## APPENDIX A: SUPPLEMENTARY FIGURES

### A1 Posterior distributions of orbital solutions

Figure A1 the posterior distribution of orbital parameters using both the RV time series and speckle imaging astrometry. Figures A2 and A3 the posterior distributions of the full joint solution using RV, speckle astrometry and the absolute proper motions.

### A2 The high-resolution spectrum; two full pages

We present in Figures A5 and A6 the high resolution ( $R \approx 20,000$ ) spectrum obtained with the TIGRE telescope.

## APPENDIX B: SELECTION AND MATHEMATICS OF THE MOVING GROUP

In order to do a five-dimensional search for stars possibly connected with Albireo kinematically, the search space should be centred on the most trustworthy spatial location (i.e. in particular parallax) and space velocity of the Albireo triple system. For this purpose we use the HIPPARCOS (2007) parallax and proper motion of Albireo B. For the search intervals we chose  $\pm 0.3$  mas in parallax (corresponding to the distance range from about 117.5 pc to 126 pc) and  $\pm 1$  km s $^{-1}$  in the two velocity coordinates (corresponding to 1.7 mas yr $^{-1}$  at 122 pc). We restricted the search to *Gaia* DR2 stars with  $G < 19$  (i.e. to  $M_G < 13.5$ ), so that the DR2 uncertainties in the measured parallaxes and proper motions are smaller than the search tolerances.

In this way we found the four stars listed in Table 9. To estimate whether these can be chance field stars, the actually found number of four stars is to be compared with the expected number from the general galactic field. The following considerations define a conservative estimate.

The expected number of stars to be found in a given 5-dimensional phase space volume of the local galactic disk simply is:

$$dN = \frac{dN}{dV} \Delta V \frac{dN}{dv_{t\alpha}} \Delta v_{t\alpha} \frac{dN}{dv_{t\delta}} \Delta v_{t\delta} \quad (\text{B1})$$

where:

- $\frac{dN}{dV}$  is the total local number density of stars
- $\Delta V$  is the 3-dimensional spatial volume under consideration
- $\Delta v_{t\alpha}, \Delta v_{t\delta}$  are the intervals under consideration in tangential
- velocity  $v_t$  in the directions of right ascension  $\alpha$  and declination  $\delta$ , respectively.

- $\frac{dN}{dv_{t\alpha}}$  and  $\frac{dN}{dv_{t\delta}}$  are the normalised densities in these velocity
- coordinates, at the specific velocities under consideration.

The canonical value for  $\frac{dN}{dV}$  can be taken from the Catalogue of Nearby Stars (CNS4). It is 0.12/(pc) $^3$ . The spatial volume  $\Delta V$ ,

defined by the above parallax tolerance and a circular field on the sky around Albireo with angular radius  $r$ , can be computed as follows:

$$\Delta V = 4\pi D^2 \Delta D * \Omega / (4\pi) \quad (\text{B2})$$

where  $D$  is the mean distance of the volume (120 pc),  $\Delta D$  is the adopted distance range (8.5 pc, see above) and  $\Omega = \pi r^2$  is the solid angle subtended by the sky field under consideration.

For the normalised densities in the velocity coordinates we conservatively assume that the space velocity of Albireo B is close to the mean galactic disk rotation. Thus we can use the normalised density close to the center of the local velocity ellipsoid, which for a Gaussian distribution of dispersion  $\sigma$  is  $(\sqrt{2\pi}\sigma)^{-1}$ . Adopting — again very conservatively — a value of  $\sigma = 10$  km s $^{-1}$  (which is true only for very young stars), we find 0.017 and 0.37 as the expected number of stars in circular sky fields of 0.8 degrees and 3.7 degrees radius around Albireo. Simple Poisson statistics then yield the probabilities given in Section 5 for finding three and four stars, respectively within these circular fields.

No further stars were found out to five degrees radius. Also, no further ones were found in a four times larger search box in  $v_{t\alpha}, v_{t\delta}$  space. The above conservative expected number of stars in this larger box would be about 0.07, 1.5 and 2.7 for  $r = 0.8$  degrees, 3.7 degrees and 5 degrees, respectively. The fact that indeed no further stars are found in the larger phase space volume lends further credibility to the reality of the moving group and confirms the conservative nature of the above calculations.

This paper has been typeset from a  $\text{\LaTeX}$  file prepared by the author.

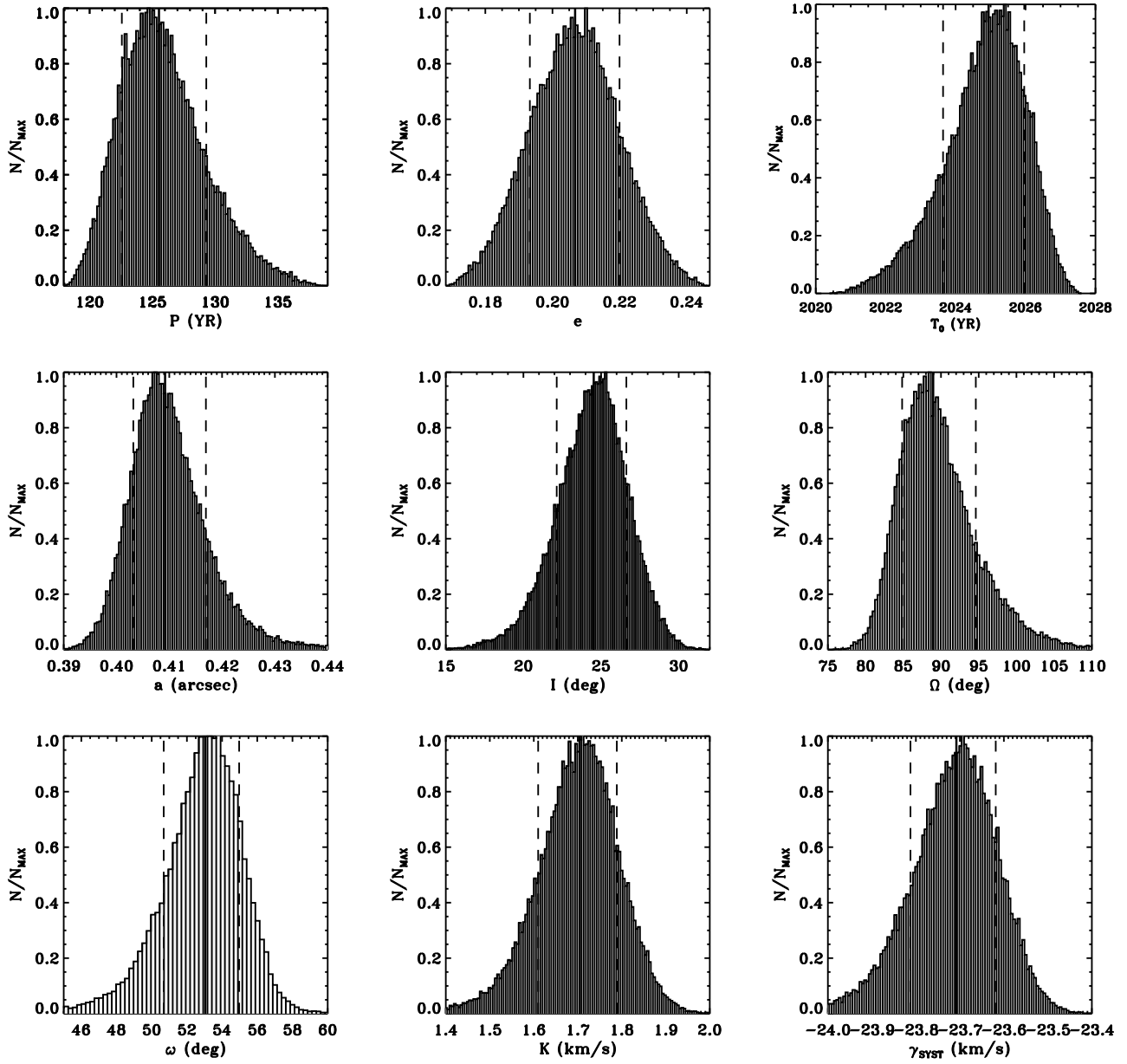


**Figure A1.** Posterior distributions of the fitted and derived parameters of the Keplerian model applied to the combination of the RV time series and speckle imaging astrometry (Table 7). The vertical dashed lines denote the 16 th and 84 th percentiles, while the vertical solid lines identify the median values.

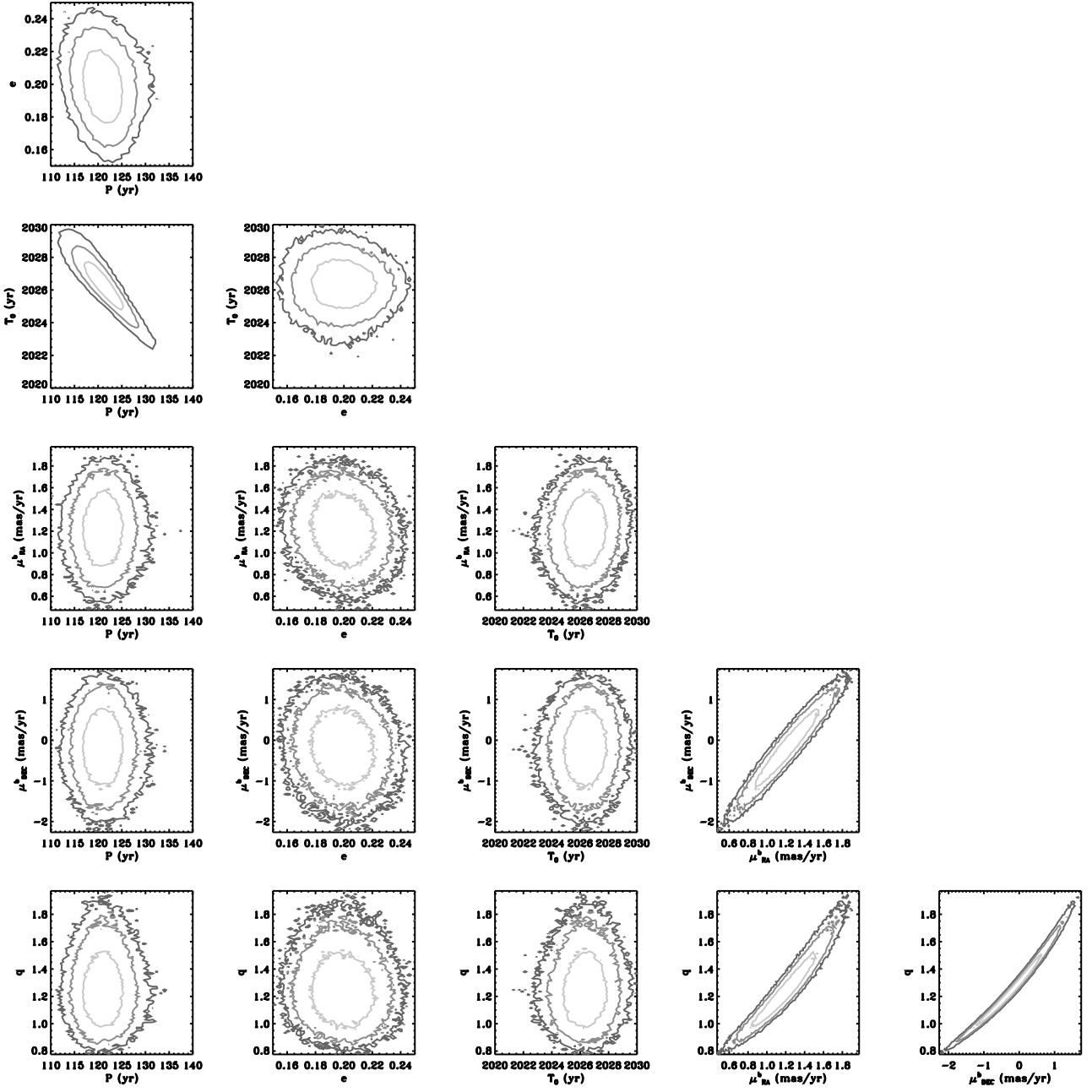
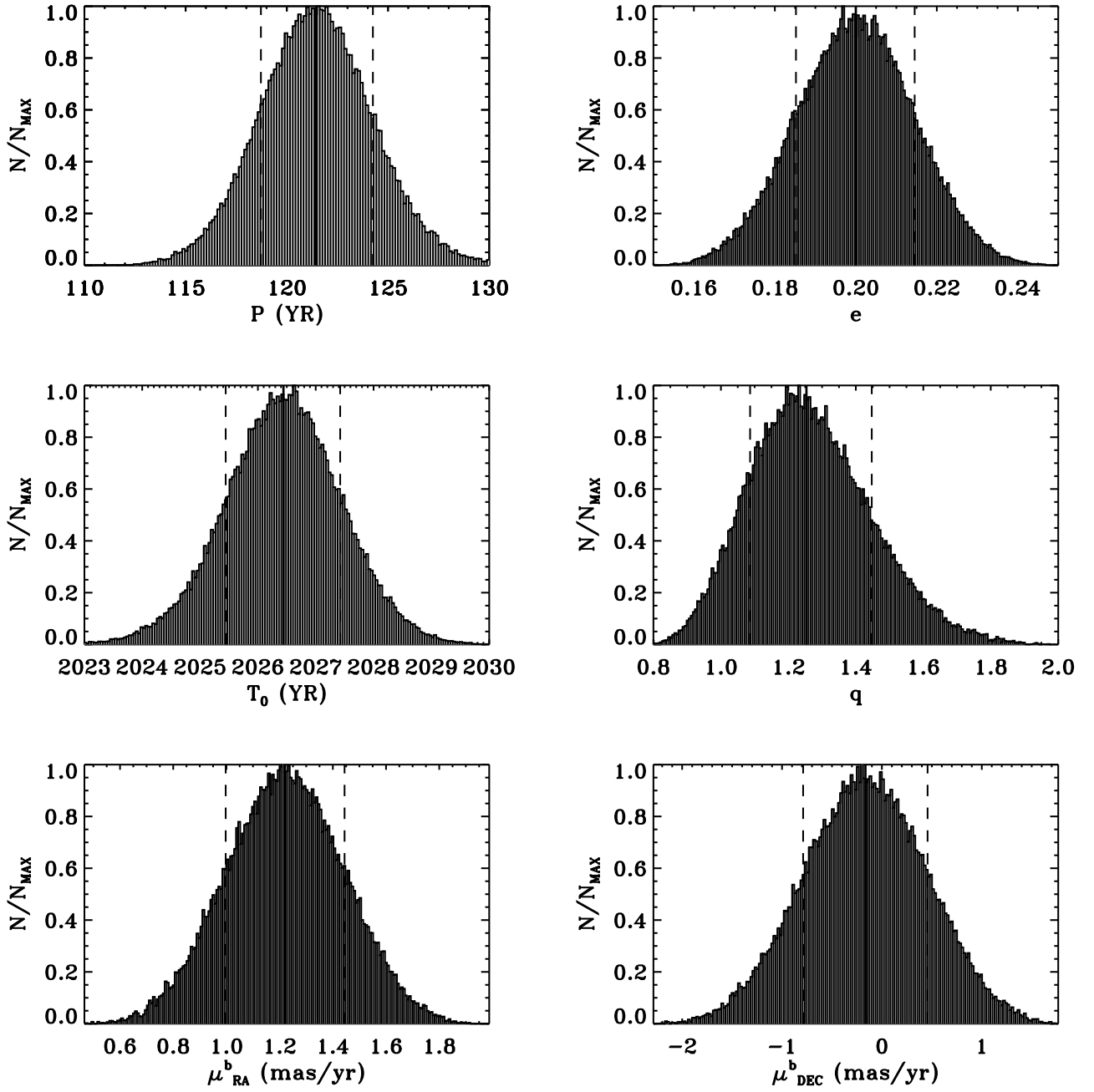
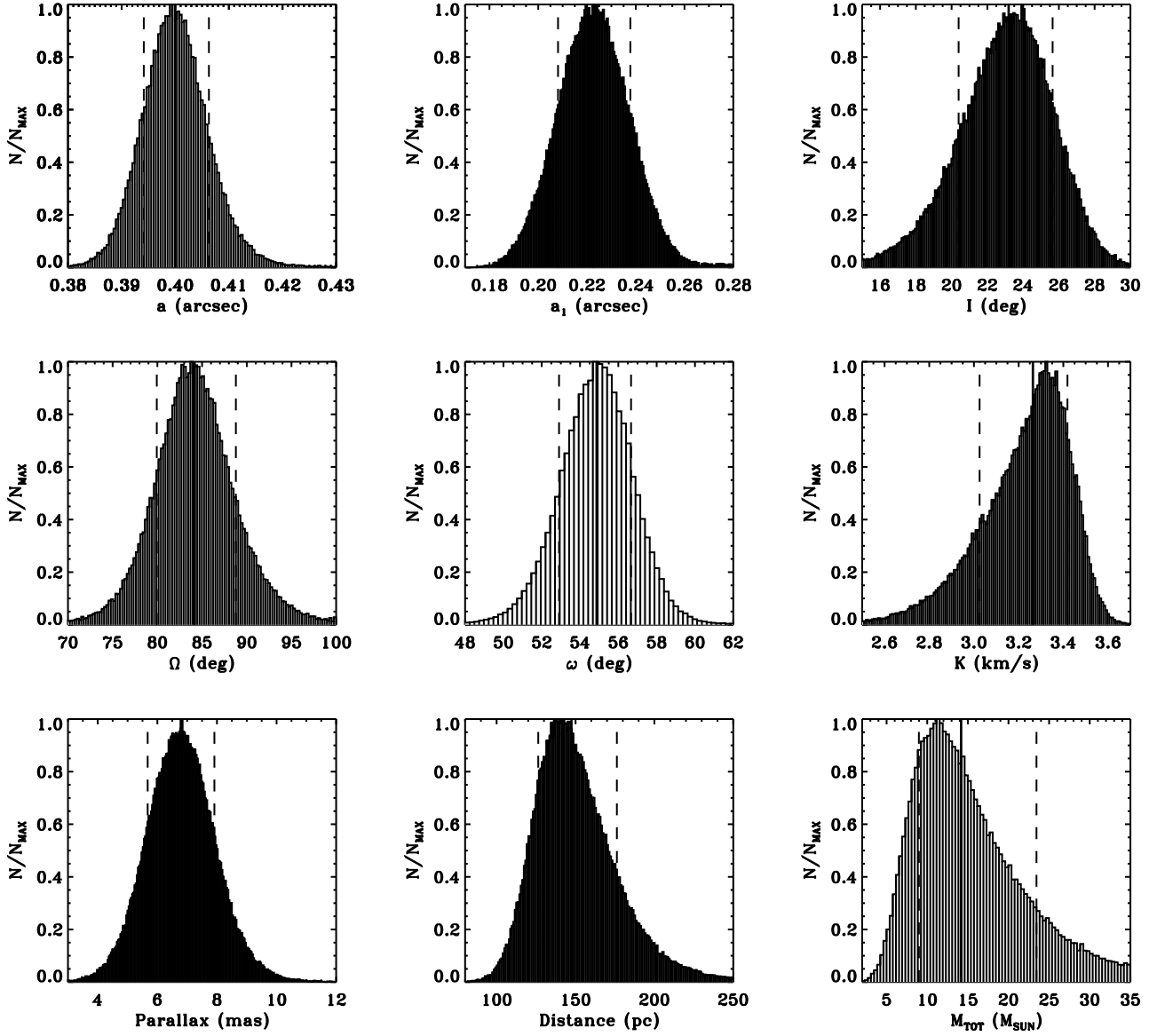


Figure A2. Joint posterior distributions for the model parameters explored in our DE-MCMC analysis (Table 8). Light grey contours indicate  $1 - \sigma$  ranges, while grey and dark grey contours indicate  $2 - \sigma$  and  $3 - \sigma$  ranges, respectively.



**Figure A3.** Posterior distributions of the four jump parameters of the Keplerian model for  $\beta$  Cyg A based on the combination of the RV time series, speckle imaging and absolute astrometry from HIPPARCOS and *Gaia* (Table 8). Same line coding as in Figure A1.





**Figure A4.** Posterior distributions of the derived parameters of the Keplerian model, parallax, and total system mass for  $\beta$  Cyg A based on the combination of the RV time series, speckle imaging and absolute proper motions from HIPPARCOS and *Gaia*. Same line coding as in Figure A1.

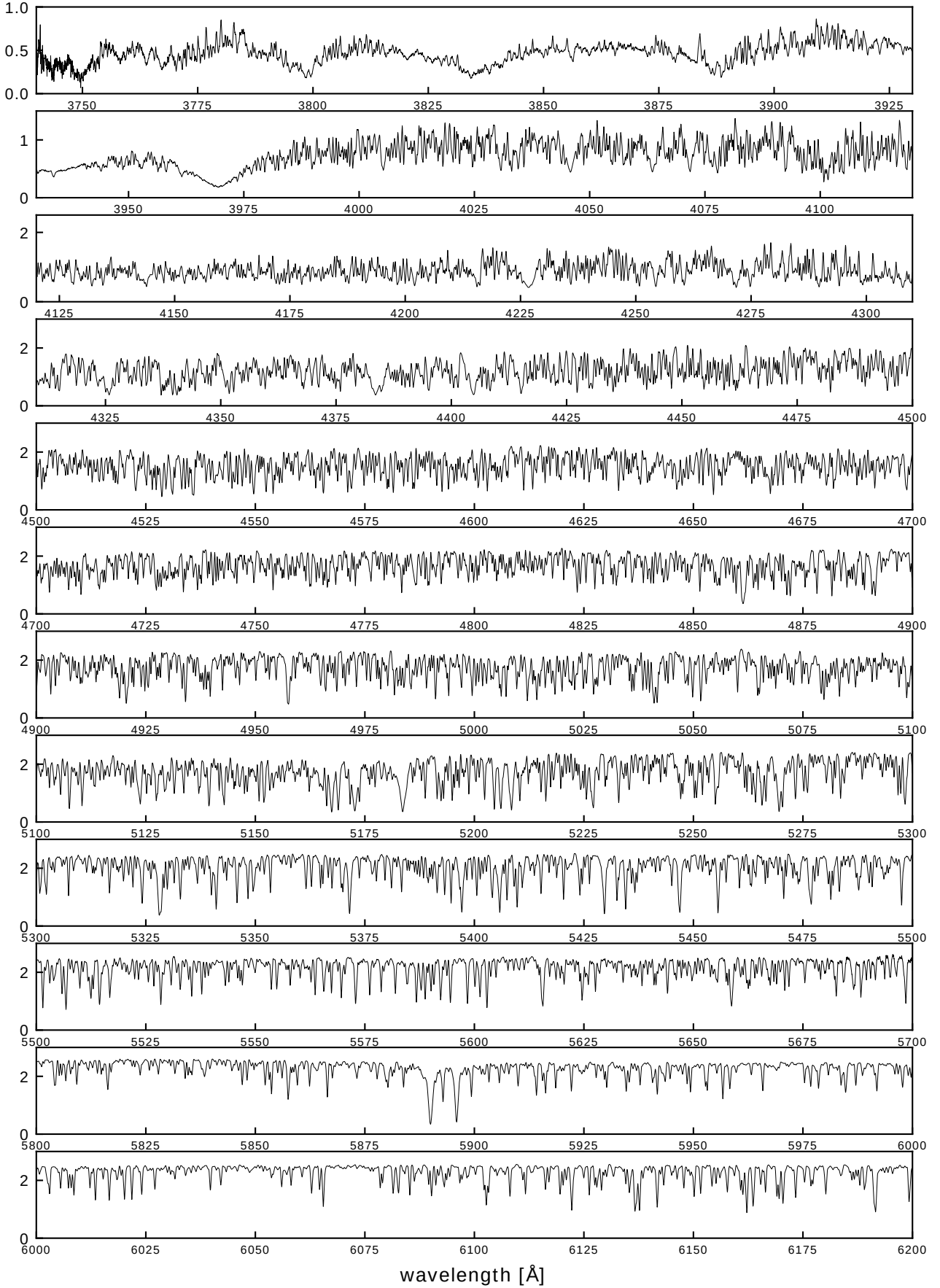


**Figure A5.** Blue part of the high resolution composite spectrum of  $\beta$  Cyg Aa and  $\beta$  Cyg Ac.

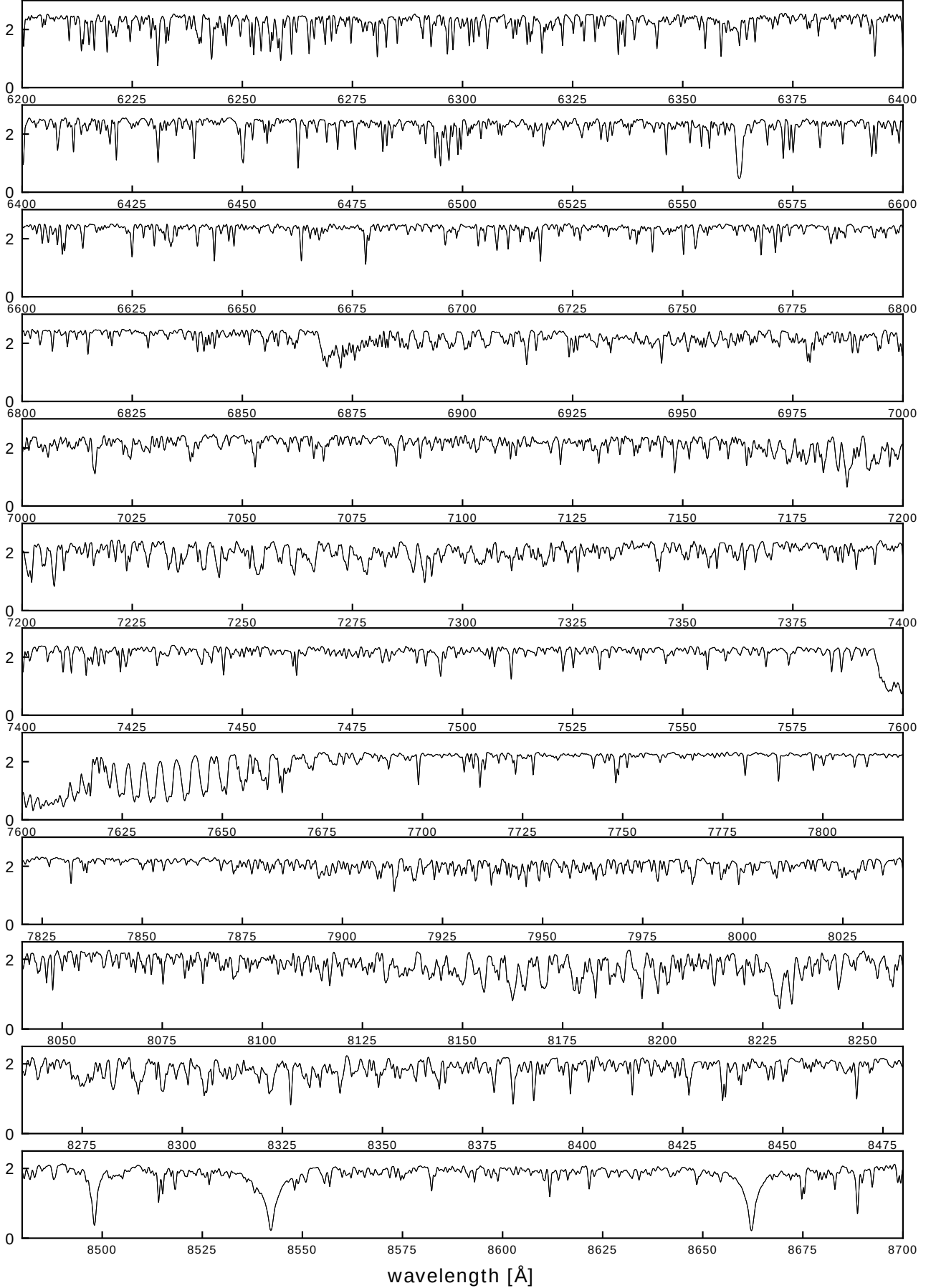


**Figure A6.** Red part of the high resolution composite spectrum of  $\beta$  Cyg Aa and  $\beta$  Cyg Ac.